Paradoxidid trilobites from a mid-Cambrian (Series 3, stage 5) limestone concretion from Jämtland, central Sweden

ADRIAN W.A. RUSHTON, THOMAS WEIDNER & JAN OVE R. EBBESTAD

This paper describes the morphology and discusses the taxonomy of the paradoxidid trilobites present in the moult ensemble described by Ebbestad *et al*. (2013) from a huge limestone concretion of the Alum Shale Formation collected at Östnår, Jämtland. Two species, both represented by numerous but small complete holaspid specimens are described as new: *Eccaparadoxides*? *thorslundi* sp. nov. is distinctive, but its generic position is considered doubtful; *Hydrocephalus spinulosus* is similar to *H. vikensis* Rushton & Weidner, 2007 (also present as a rarity in the moult ensemble) and is partly distinguished from it by characters of the thorax. Also illustrated are a few specimens that have been collected at various localities between Hackås and Brunflo. They appear to represent individuals of some of the species in the moult ensemble and are about twice the size of their type specimens. • Key words: Cambrian, stage 5, Jämtland, Sweden, *Eccaparadoxides*, *Hydrocephalus*, morphology, taxonomy.

Adrian Rushton (corresponding author), The Natural History Museum, Cromwell Road, SW7 5BD London, U.K.; A.Rushton@nhm.ac.uk • Thomas Weidner, Ravnholtvej 23, Rårup, 7130 Juelsminde, Denmark • Jan Ove R. Ebbestad, Museum of Evolution, Uppsala University, Norbyvägen 16, SE 752 36 Uppsala, Sweden

In 2006 the Museum of Evolution, Uppsala University, acquired a large fossiliferous bituminous limestone block (here referred to as the "Big Block") found at the abandoned Tännberget alum shale quarry at Östnår, near Hackås, about 35 km south of Östersund in Jämtland, central Sweden (Ebbestad *et al.* 2013); see Fig. 1. Münder (2007, p. 144) reported the discovery of the concretion and illustrated a few of the contained trilobites. A bedding-plane, roughly 80 cm by 50 cm within the "Big Block", the "principal surface", is remarkable for displaying over 90 paradoxidid trilobites (Ebbestad *et al.* 2013), together with 56 agnostoids (Weidner & Ebbestad 2014). Ebbestad *et al.* (2013) described the fauna on the principal surface as a moult ensemble, and they illustrated the disposition of the paradoxidids and discussed their ecology and moulting behaviour. Discussion of their taxonomy was deferred, and it is the aim of the present paper to offer such discussion.

Nearly all of the paradoxidid exoskeletons are wholly or partly articulated, many being complete dorsal shields or axial shields (*i.e.* exoskeletons that lack the librigenae). Ebbestad *et al.* (2013, p. 22) interpreted the exoskeletons as moulted configurations. The preservation is generally good; most specimens are in some relief, retaining part of their original convexity, but there has been slight diagenetic compaction, particularly the crushing of the anterior parts of the glabella onto the underlying hypostome, as discussed by Ebbestad *et al.* (2013, p. 20). All of the complete paradoxidid exoskeletons on the principal surface are holaspids in that they have the full number of free thoracic segments, while the pygidia do not bear unreleased segments and thus do not resemble transitory pygidia. However, most are comparatively small, having exoskeletons between 20 mm and 40 mm long. They do not show obvious features of meraspids, such as a long preglabellar field or greatly elongated pleural spines to the second thoracic segment, but they are considered to be relatively immature specimens, and likely much smaller than the size that they might ultimately be expected to attain. In addition to the "Big Block", specimens of the three species discussed herein have been collected from other concretions at Tännberget quarry and at other localities between Hackås and Brunflo (Fig. 2). Although those may include parts of larger exoskeletons, they are mostly fragmentary or ill-preserved. All material derives from the *Acadoparadoxides pinus – Pentagnostus praecurrens* Zone of the *Acadoparadoxides* (*Baltoparadoxides*)

Figure 1. Tännberget quarry, Östnår near Hackås, summer 2015, showing autochthonous Alum Shale with large concretions. The largest block in the foreground is about 1 metre long.

oelandicus Superzone (Fig. 3) and was collected in Jämtland from autochthonous strata.

Problems with the taxonomy of *Paradoxides*

Paradoxides sensu lato is a large genus. Various workers have attempted to group the numerous species into genera or subgenera, as listed by Dean & Rushton (1997), but those attempts have not met with general acceptance. Difficulties have been highlighted by Geyer & Landing (2000), Fletcher *et al*. (2005) and Geyer & Vincent (2014); these include the incomplete knowledge of the exoskeleton of several species, a general lack of knowledge of the ontogeny in most species, and the difficulty of distinguishing convincing apomorphic features that could enable the characterisation of natural clades. We agree with the observation by Geyer (1993) that a paradoxidid species cannot well be characterised without knowledge of, at the least, the whole cranidium and the associated pygidium, and in the present paper we also draw attention to features of the thorax. Regarding ontogeny, there are two main problems. One is that the early growth stages that might provide striking ontoge-

netic features (as in *Hydrocephalus carens* Barrande; Šnajdr 1958, figs 23, 24) are seldom found and are known only in very few species. The other is that the growth-trajectory in paradoxidids is unusually long, such that a species may grow from a small holaspid to a well grown form that is 10 or even 15 times as long (see Šnajdr 1987, p. 99). To be able to refer specimens of such different sizes with confidence to a single species may require favourable occurrence and preservation; nevertheless, from published accounts over many years (Barrande 1852, Westergård 1936, Esteve 2014) it is quite evident that small holaspid specimens of a paradoxidid species can be recognised as conspecific with much larger examples in those cases where the holaspid growth is largely isometric, and provided that sufficient specimens are available. The large-scale investigation by Esteve (2014, figs 16, 17) showed several isometric trends in the growth of cranidia of *Eccaparadoxides pradoanus* and some allometric trends, particularly in the smaller growth stages (Esteve 2014, fig. 15B).

The paradoxidids from the "Big Block" provide a fairly large sample of relatively complete and well-preserved specimens that allow a thorough description of the species present, although over only a small size-range. The two
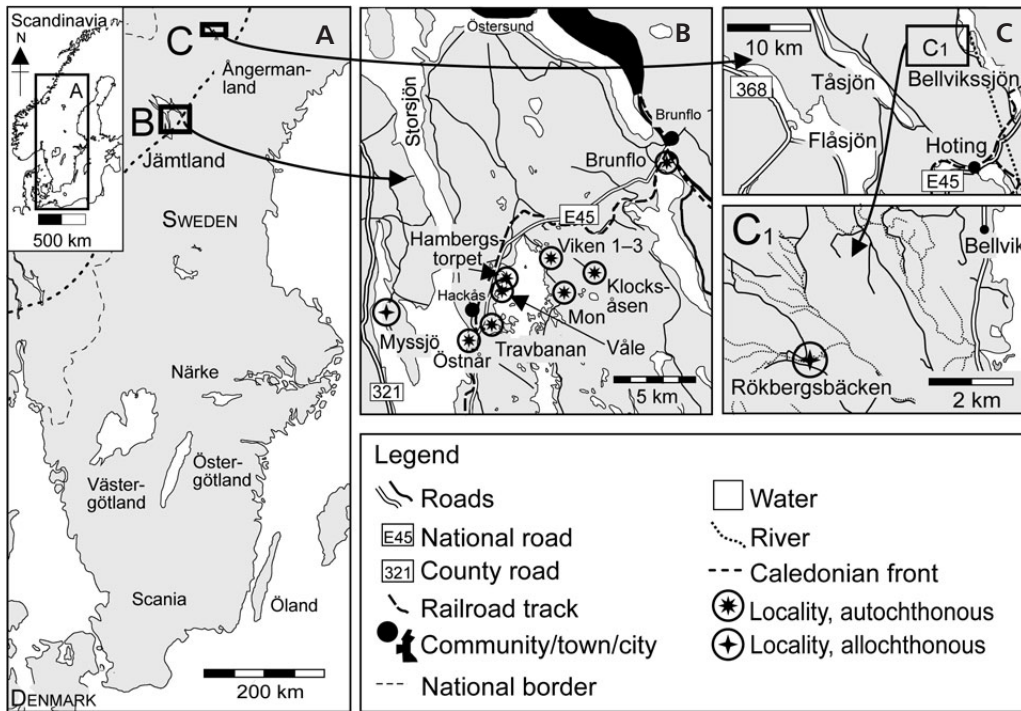
Figure 2. Locality map of south and central Sweden (A), with details of fossil localities in Jämtland (B) and Ångermanland (C).

Chrono-stratigraphy			Trilobite superzones	Polymerid trilobites	Agnostoid zones
System	Series	Stage			
Cambrian	Cambrian Series 3	Guzhangian	*Paradoxides (Paradoxides) forchhammeri*	*Simulolenus alpha*	*Agnostus pisiformis*
				not defined	*Lejopyge laevigata*
				Solenopleura? brachymetopa	
		Drumian	*Paradoxides (Paradoxides) paradoxissimus*	*Paradoxides davidis* (not defined)	*Goniagnostus nathorsti*
					Ptychagnostus punctuosus
				Bailiella ornata	*Acidusus atavus* u / l
		Stage 5		*Ctenocephalus exsulans*	*Triplagnostus gibbus*
			Acadoparadoxides (Baltoparadoxides) oelandicus	*Acadoparadoxides pinus*	*Pentagnostus praecurrens*
				Eccaparadoxides insularis	no agnostoid zones

Figure 3. Biostratigraphical divisions of the mid-Cambrian Series 3 in Scandinavia, after Weidner & Nielsen (2015).

Table 1. Estimates of mean lengths of cranidia and complete specimens of the three paradoxidid taxa from the principal surface of the "Big Block". The number in parentheses for the mean length of complete specimens gives the number of specimens measured. All lengths are in mm.

Taxon	*E.? thorslundi*	*H. spinulosus*	*H. vikensis*
Total No. of specimens	51	36	2
No. of specimens measured	33	28	2
Mean length of cranidium	10.3	8.2	10.8
Standard deviation	4.56	2.17	1.14
Mean length of complete specimens	35.2 (19)	26.0 (9)	32.8 (1)

most common species, when found complete, show features that differ from described species, and we have named them here as new. We recognise, however, that neither of the new forms have well-marked apomorphies in the cephalon or pygidium, and it may therefore prove difficult to assign isolated sclerites to these species, or to distinguish them from existing species that have so far been described only from isolated cranidia or pygidia. It may seem unsatisfactory to base new species on small holaspid specimens, but we contend that the holotypes of the two new species are sufficiently well supported by the host of paratype specimens on the principal surface of the "Big Block", and these allow an assessment of the consistency of their features, and the morphological variation they display.

Statistical analyses

General. – The principal surface of the "Big Block" contains 146 identified specimens of which 51 are recognized as *Eccaparadoxides*? *thorslundi* sp. nov., 36 as *Hydrocephalus spinulosus* sp. nov., 2 as *H. vikensis* Rushton & Weidner, 2007, 1 as *Ellipsocephalus* sp., and 56 as the agnostoid *Pentagnostus praecurrens* (Westergård, 1936) (Figs 4, 5; Table 1). The morphological variation of, and among, the cranidia was analysed with a set of 12 linear measurements for each specimen (Fig. 6, Tables 1–6). For each taxon some additional specimens outside the "Big Block" were also measured and some cranidia of *E. pusillus* (Barrande, 1846) and *E. insularis* (Westergård, 1936) were measured for comparison with *E.? thorslundi*. Very precise measurements were possible from digital images of the specimens stored at PMU, while other taxa were largely measured from images in the original publications. In total 33 cranidia of *E.? thorslundi*, 28 cranidia of *Hydrocephalus spinu-*

losus and 2 cranidia of *H. vikensis* were measured (Tables 1–6). In addition the relative length to width proportions of pygidia was measured in 17 specimens of *H. spinulosus* to aid the taxonomic description. The length of complete specimens was measured for 19 specimens of *E.? thorslundi*, 9 specimens of *H. spinulosus* and 1 specimen of *H. vikensis*.

The smallest specimen of *E.? thorslundi* on the principal surface has a cranidial length of 2.9 mm and the largest has a cranidial length of 18.4 mm. Note that the second largest specimen has a cranidial length of only 13.8 mm. The mean cranidial length of all specimens is 10.3 mm. The length of complete specimens ranges between 20.1–58.9 mm with a mean length of 35.2 mm. Similar measurements for *H. spinulosus* give a length of 3.5 mm for the smallest cranidium and 11.7 mm for the largest, with a mean cranidial length of 8.2 mm. Complete specimens range in size between 17.4 –32.1 mm with a mean length of 26.0 mm. The two specimens identified as *H. vikensis* have cranidial lengths around 10 mm and the single complete specimen is 32.8 mm long (see summary in Table 1).

The data sets were analysed using PAST version 3.10 (Hammer *et al*. 2001).

Bivariate analysis. – Some of the bivariate plots and statistics are shown in Figs 7 and 8. These were selected on the basis of the Principal Component Analysis, representing the parameters with the greatest variability. Reduced major axis regression was used to test whether the regression slopes of the various taxa differed significantly from each other. The basic assumption was that the slopes were similar, with a significance level of $p < 0.05$.

Fig. 7 shows the three species of *Eccaparadoxides*. Fig. 7A shows a greater increase of the width across the eyes (W3) during growth as the length (L1+L2) increases. Although there are differences in the regression slopes of the three species the difference is not statistically important. The maximum width of the glabella (W1) (Fig. 7B) increases more than the width of the occipital lobe (W2) during growth, but once again there is no statistical difference among the analysed species. Only about 30% of the variability in *E. insularis* is explained by the maximum width of the glabella. When the maximum width δ–δ across the eyes (W3) is plotted against the width across the preocular genae (W7) (Fig. 7C), a statistical difference exists between the slope of *E.? thorslundi* relative to that of *E. pusillus*. This is not surprising considering the narrow preocular genae of *E. pusillus*. The relationship between

---

Figure 4. Photograph (upper) of the principal surface of the "Big Block" (PMU 25711), with an explanatory drawing of the specimens (lower) with added sub-numbers (PMU 25711/1–25711/101). The stippled square indicates the detail shown in Fig. 5. Updated and modified from Ebbestad *et al*. (2013).
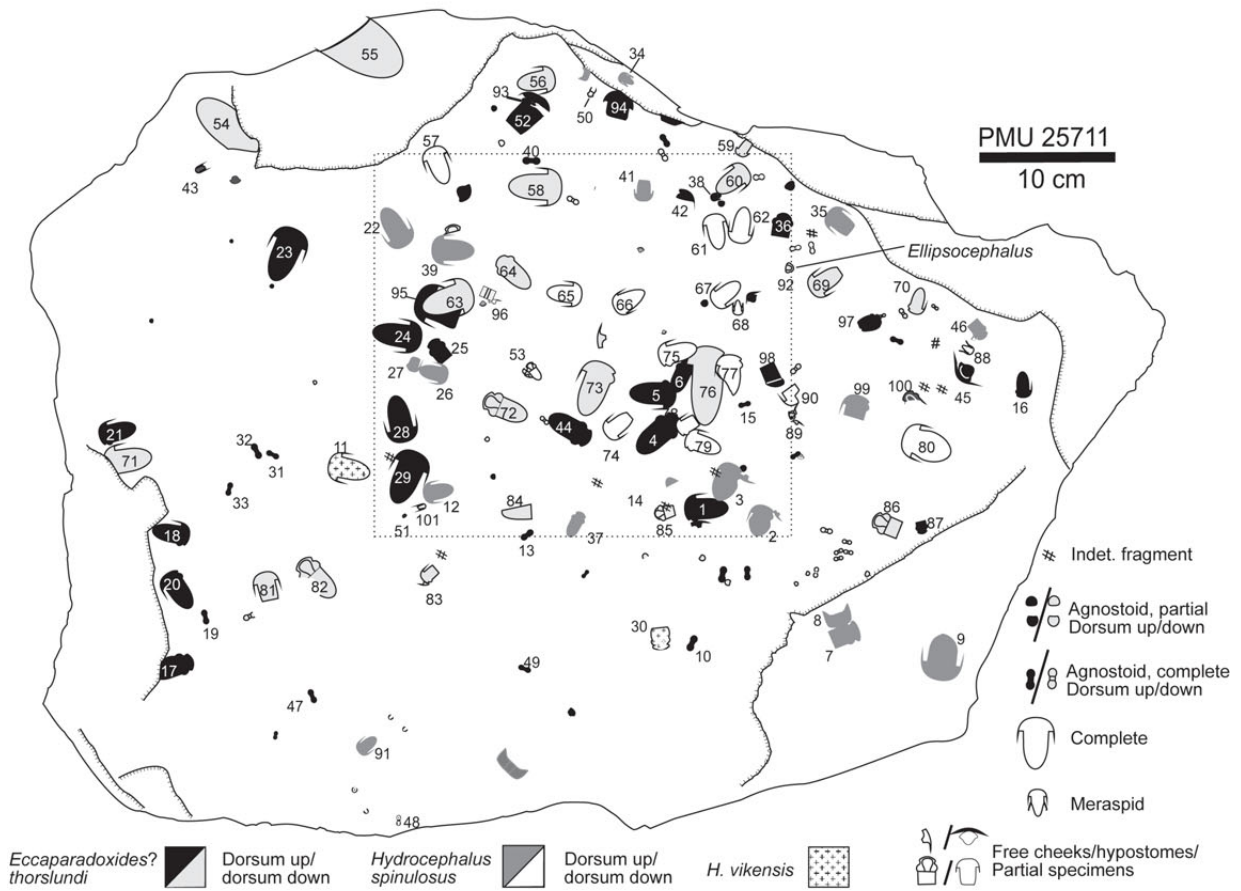
PMU 25711

10 cm

Ellipsocephalus

Indet. fragment

Agnostoid, partial
Dorsum up/down

Agnostoid, complete
Dorsum up/down

Complete

Meraspid

Free cheeks/hypostomes/
Partial specimens

Eccaparadoxides?
thorslundi   Dorsum up/
dorsum down

Hydrocephalus
spinulosus   Dorsum up/
dorsum down   *H. vikensis*

Table 2. Measurements on cranidia of *E.? thorslundi*. See Fig. 6 for explanations of the parameters. A '**J**' following the specimen number indicates a juvenile specimen. An '**H**' following the specimen number indicates the holotype.

Specimen	L1+L2	L1	L2	Border	PGF	L3	L4	W1	W2	W3	W6	W7
PMU 25564	9.2	8.1	1.1	0.6	0.5	4.7	0.6	6.2	3.9	12.2	2.9	10.8
PMU 25997	27.9	26.2	1.7	1.6	0.1	14.6	2.6	18.4	13.5	35.3	7.8	33.8
PMU 25711/1	11.1	9.7	1.4	0.7	0.7	6.7	0.4	7.9	5.3	15.9	3.7	14.9
PMU 25711/4	13.6	12.2	1.4	1.4	–	7.2	1.4	8.8	6.7	18.2	4.9	16.3
PMU 25711/5	13.2	11.6	1.6	1.2	0.4	6.6	0.8	7.6	5.5	15.2	4.8	15.1
PMU 25711/6	9.2	8.2	1.0	0.6	0.4	5.0	0.6	6.1	3.9	13.5	3.9	12.0
PMU 25711/16	7.3	6.3	1.0	0.6	0.4	3.2	0.5	4.4	2.7	9.1	–	8.1
PMU 25711/17	13.8	12.1	1.7	0.9	0.8	7.0	1.1	8.3	5.9	17.5	4.3	16.4
PMU 25711/18	10.4	9.1	1.3	0.6	0.7	6.1	0.8	6.6	4.9	14.5	3.7	12.0
PMU 25711/20	10.8	9.4	1.4	0.7	0.7	5.4	0.9	7.2	5.1	15.2	–	14.2
PMU 25711/21 **J**	7.6	6.6	1.0	0.5	0.5	4.1	0.5	4.5	3.2	9.8	–	8.7
PMU 25711/23	13.4	12.3	1.1	0.7	0.4	6.8	1.4	9.1	6.2	18.4	–	16.6
PMU 25711/24	11.0	10.2	0.8	–	–	5.8	1.2	8.1	5.2	14.8	3.8	12.5
PMU 25711/25	8.4	7.6	0.8	0.6	0.2	4.7	0.8	5.6	4.0	12.1	–	10.7
PMU 25711/28 **J**	12.0	10.9	1.1	0.8	0.3	6.6	1.4	8.4	5.5	16.0	–	15.1
PMU 25711/29 **H**	13.8	12.1	1.7	1.7	–	6.9	1.2	9.1	6.0	21.0	–	19.4
PMU 25711/34 **J**	5.2	4.3	0.9	0.4	0.5	2.4	0.6	2.9	1.7	4.6	1.6	5.9
PMU 25711/43 **J**	2.9	2.3	0.6	0.2	0.4	1.5	0.3	1.4	1.0	3.3	–	3.5
PMU 25711/44	11.2	10.4	0.8	0.7	0.1	5.8	0.9	7.6	4.8	15.9	4.2	13.5
PMU 25711/58	12.7	11.5	1.2	1.2	–	7.0	1.1	7.9	6.1	18.4	–	15.6
PMU 25711/59	5.9	5.2	0.7	0.5	0.2	3.3	0.4	3.7	2.6	8.3	–	7.1
PMU 25711/60	9.6	9.1	0.5	0.5	–	5.1	0.9	6.9	4.9	14.5	–	11.5
PMU 25711/63	12.7	10.9	1.8	0.8	1.0	6.9	0.9	8.9	6.2	17.6	–	16.7
PMU 25711/64	10.2	8.2	2.0	0.6	1.4	4.9	0.5	5.4	4.2	12.5	3.1	11.3
PMU 25711/69	10.8	9.4	1.4	0.7	0.7	5.6	0.9	7.1	4.7	13.5	3.5	12.2
PMU 25711/70	7.8	6.9	0.9	0.5	0.4	4.3	0.6	4.7	3.5	10.2	–	9.3
PMU 25711/72	11.6	11.2	0.4	0.4	–	6.2	1.0	7.0	4.9	14.7	–	12.8
PMU 25711/73	12.3	11.0	1.3	0.7	0.6	6.4	1.0	7.7	5.2	16.2	–	15.0
PMU 25711/76	18.4	17.6	0.8	0.8	–	–	–	13.0	8.6	23.8	–	19.6
PMU 25711/81	9.0	8.0	1.0	1.0	–	4.4	1.6	6.1	4.2	12.0	3.0	11.7
PMU 25711/83 **J**	7.2	6.6	0.6	0.5	0.1	3.6	0.5	4.1	2.9	8.9	–	8.6
PMU 25711/85	7.7	6.6	1.1	0.5	0.6	4.0	0.6	4.1	3.2	9.5	–	8.2
PMU 25711/149	20.5	18.8	1.7	1.7	–	11.4	2.0	13.3	9.4	25.9	–	25.5

Table 3. Measurements on cranidia of *E. pusillus*. See Fig. 6 for explanations of the parameters.

Specimen	L1+L2	L1	L2	Border	PGF	L3	L4	W1	W2	W3	W6	W7
MŠ 437	25.5	23.5	1.8	1.8	–	15.0	2.2	18.0	13.0	35.0	8.0	27.0
NM 1.4735	14.5	13.7	0.8	0.8	–	10.0	1.0	10.5	9.3	19.0	4.0	15.5
MŠ 435	13.0	12.0	1.0	1.0	–	6.5	1.5	8.0	5.5	15.0	3.5	11.5
Akc.36675	11.5	11.0	0.5	0.5	–	7.0	2.0	7.5	5.0	16.4	4.5	–
MŠ 456	6.5	5.5	0.5	0.5	–	3.0	0.4	4.2	3.0	8.5	2.0	7.5

the widths W3 and W7 is otherwise nearly isometric for *E.? thorslundi* and *E. insularis*. In Fig. 7D the length of the glabella (L1) is plotted against the length of the palpebral lobe (L3). In *E. insularis* the lobes are getting shorter relative to the glabellar length and the differences in the slopes are statistically significant.
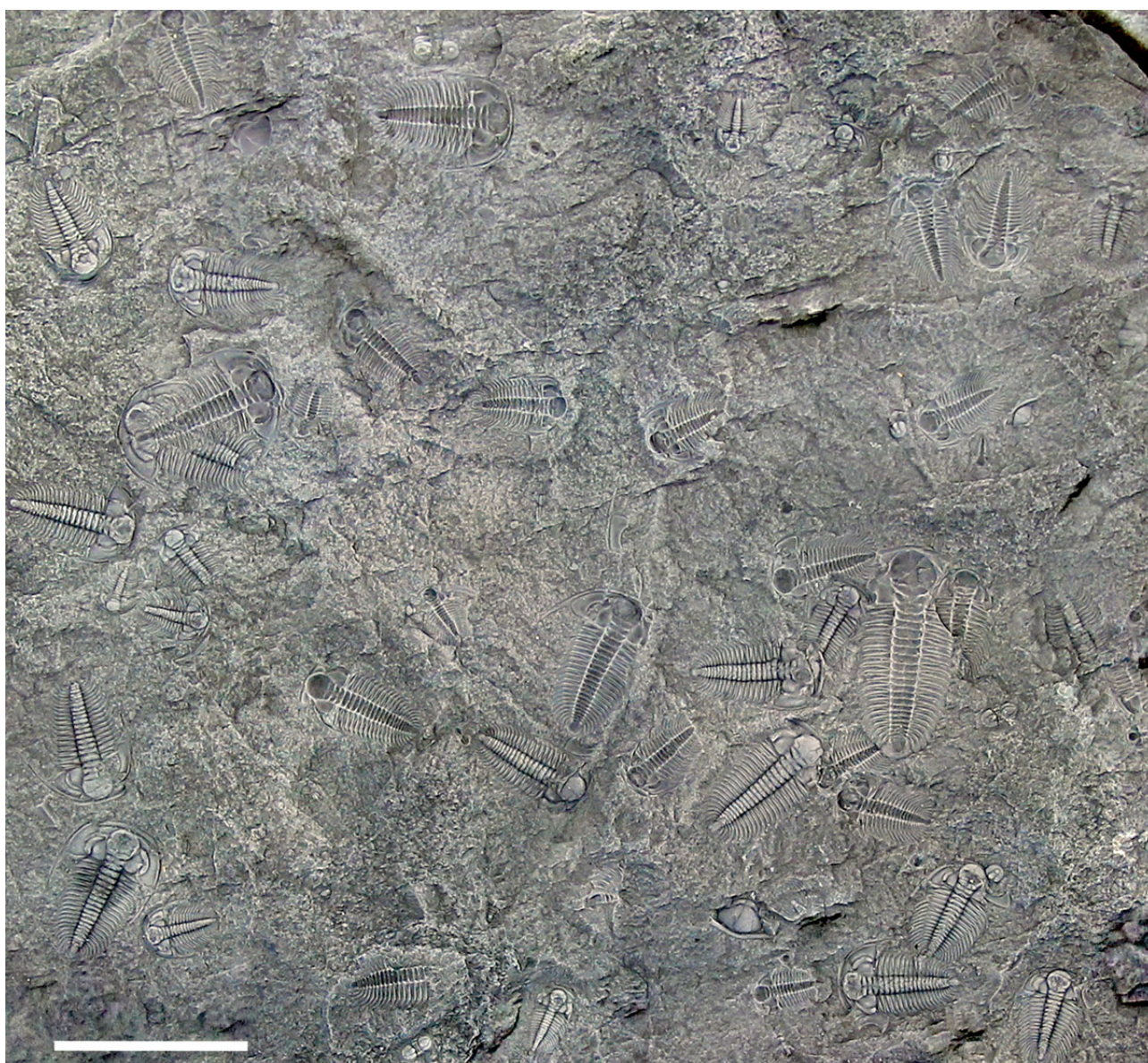
Figure 5. Detail of the principal surface of the "Big Block" showing the random distribution and the presence of specimens with dorsum up or dorsum down. See Figure 4 for position on the principal surface. Scale bar = 5 cm.

The same sets of bivariate plots are shown for *Hydrocephalus spinulosus* and *H. vikensis* (Fig. 8). In Fig. 8A the width across the eyes (W3) increases more than the length of the cranidium and there is no statistical difference in the two species. The very narrow occipital lobe is demonstrated in Fig. 8B, and both species follow a similar growth pattern. As with the *Eccaparadoxides* species, the length and width of the cranidium exhibits nearly isometric growths in *Hydrocephalus* (Fig. 8C). The difference between the relative length of the glabella (L1) and the length of the palpebral lobe (L3) becomes reduced during growth (Fig. 8D). The difference between *H. spinulosus* and *H. vikensis* is not significant.

Principal Component Analysis (PCA). – PCA was performed on the same 12 parameters measured for the bivariate analysis (Fig. 9, Tables 2–6). Measurements for the parameter W6 is unavailable for many specimens. Testing PCA on subsets with the available W6 measurements for *Eccaparadoxides* and *Hydrocephalus* yielded very low loadings for PC 1 and PC 2, so owing to these two factors this parameter was omitted from the main analysis. Similar reasoning applies to the length of the preglabellar field (PGF) parameter. In addition, the PGF is not developed in many specimens of *Eccaparadoxides* or, in the case of *Hydrocephalus*, is seen only in juvenile specimens. Specimens were also omitted from the analy-

Table 4. Measurements on cranidia of *E. insularis*. See Fig. 6 for explanations of the lengths and widths.

Specimen	L1+L2	L1	L2	Border	PGF	L3	L4	W1	W2	W3	W6	W7
SGU 629	5.2	4.3	0.9	0.4	0.5	2.1	0.7	3.2	2.4	6.6	1.9	6.0
SGU 693a	9.1	8.2	1.0	0.5	0.4	4.0	–	6.0	4.4	–	–	9.5
SGU 696	8.1	7.2	0.9	0.3	0.5	3.4	0.5	3.8	3.8	9.6	2.6	9.1
SGU 699	6.4	5.9	0.5	0.5	–	2.8	0.7	4.2	3.1	7.7	2.1	8.0
SGU 700	6.5	6.1	0.4	0.4	–	2.9	0.6	5.2	3.3	9.1	2.3	9.1
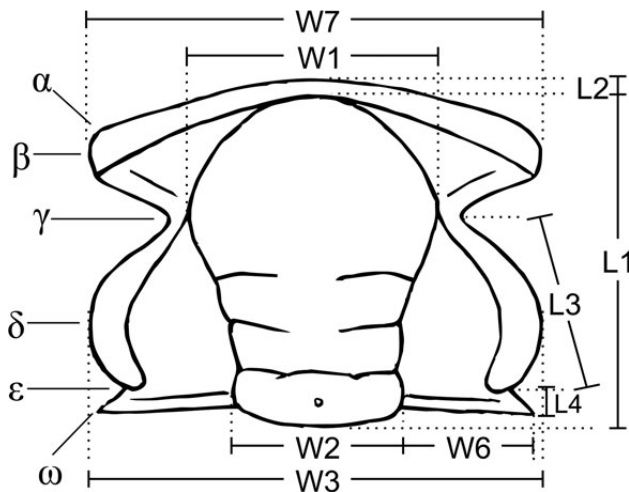
Figure 6. Outline of a paradoxidid cranidium, showing the dorsal facial suture extending from α to ω, with salient points between them used in the text, labelled β, γ, δ and ε. Cranidial measurements: L1 = the sagittal length of the glabella (including occipital lobe); L2 = the sagittal length of the frontal area. This includes the preglabellar field (PGF) and the anterior border and border furrow; L3 = the length of the eye as a chord from γ to ε; L4 = the exsagittal length of the postocular suture; W1 = the maximum width of the glabella; W2 = the width of the occipital lobe; W3 = the width across the eyes (δ–δ); W6 = the width of the postocular gena from the axial furrow to point ω; W7 = the width across the preocular genae (β–β).

sis if any of the tested parameters proved impossible to measure (see Tables 2–6).

Eccaparadoxides (Fig. 9A)

Unsurprisingly Principal Component 1 (PC 1) accounts for most of the variance, with the overall length of the cranidium and the length of the glabella increasing towards the right. Most specimens plot close to the PC 1 axis and to the left in the diagram. In the case of *E.? thorslundi* this reflects the relatively uniform size-distribution on the principal surface of the "Big Block" (Table 2) and a conservative morphology. The larger specimens of *E.? thorslundi* plotting to the right are not from the principal surface. The low loading of L2 relative to L1 demonstrates the allometric growth component, showing that the length (sag.) of the frontal area is proportionally very large in re-

lation to the overall length of the cranidium in specimens to the left in the diagram (*i.e.* juvenile to small holaspid specimens). The length of the palpebral lobes (L3) show a similar development, but the difference between their relative lengths compared to the overall length of the cranidium is smaller. The length of the glabella has larger loadings than its width parameters, showing that the glabella is broader and shorter in specimens to the left while longer and narrower in specimens to the right. As the loadings for the widths of the cranidium (W3, W7) are large, specimens to the left have a narrow cranidium with a relatively wide glabella and specimens to the right have a broad cranidium with a proportionally narrow and elongated glabella.

PC 2 shows contrasting loadings, where the anterior width (W7) and length of the glabella (L1) are the most prominent. Specimens of *E. pusillus* have high values on PC 2, reflecting their proportionally narrow anterior width. One exception is MŠ 456, a small specimen where the anterior width is proportionally wide. The narrow width therefore seems to be a derived character in *E. pusillus*, as expressed in larger specimens, while it is primitive in *E.? thorslundi*. The width of the occipital lobe (W2) is also greater in specimens with high values on the PC 2 axis and proportionally narrow in specimens plotting low on the axis. Thus, the holotype of *E.? thorslundi* plots very low, mostly owing its narrow occipital lobe. It also has proportionally long palpebral lobes relative to the length of the glabella (see loadings for L1 and L3), meaning that specimens with a high score on PC 2, like those of *E. pusillus*, have proportionally shorter glabella relative to the length of the palpebral lobes.

Hydrocephalus (Fig. 9B)

The allometric size variance along PC 1 reflects nearly equal growth in the cranidial and glabellar lengths (L1+L2, L1; the length of the glabella is essentially equal to the length of the cranidium in larger specimens) as well as a large relative growth in the width of the cranidia (W3, W7). The glabella expands less (W1, W2) than it grows in length (L1), with the maximum width of the glabella increasing more relative to the width of the occipital lobe. This means
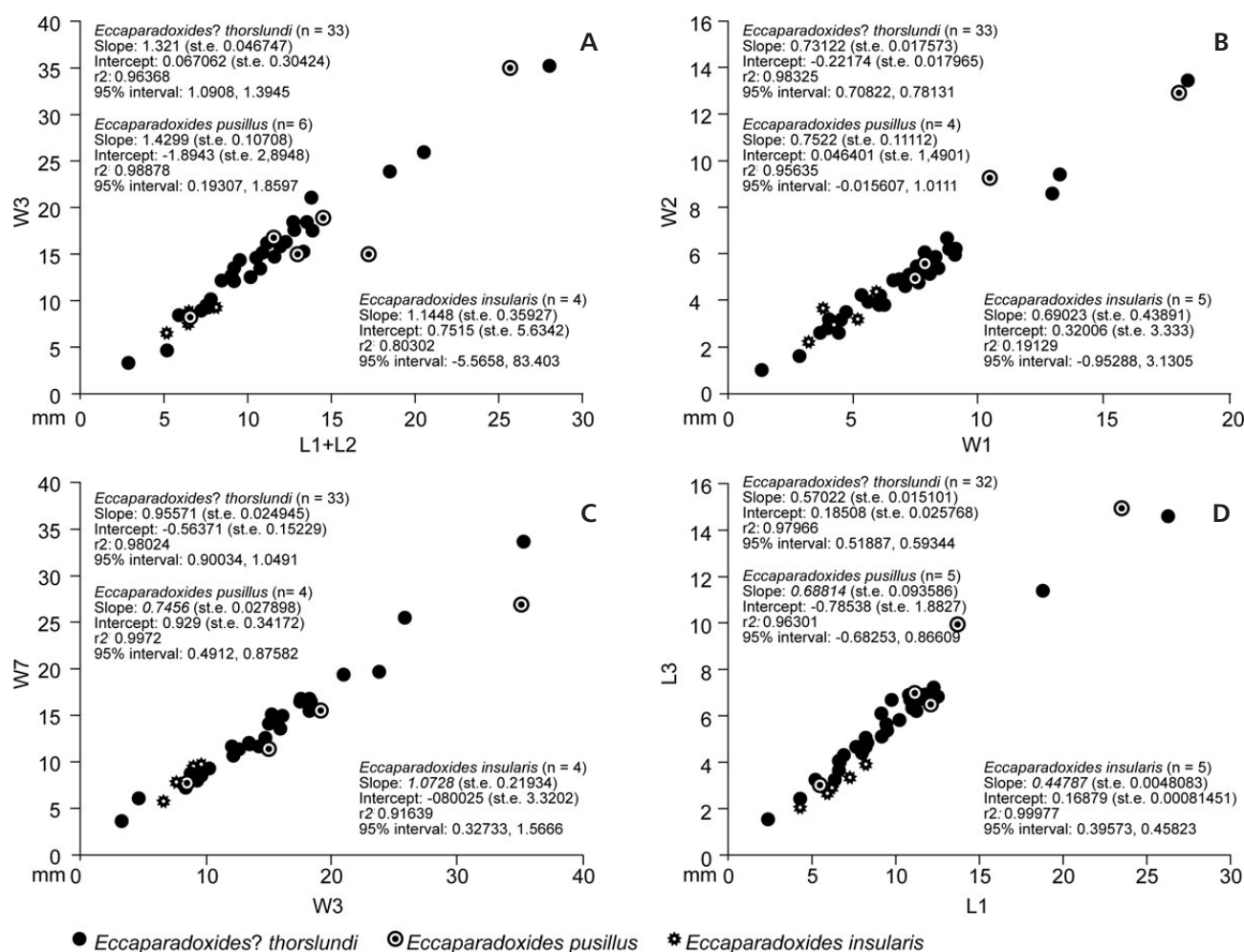
Figure 7. Bivariate plots and regression statistics of measurements made on cranidia of *Eccaparadoxides*? *thorslundi*, *E. pusillus* and *E. insularis*. The 95% confidence interval is given for the slope. St. e. = standard error. See Fig. 6 for further explanation of the measured parameters. • A – total length of cranidium (L1+L2) against width across the eyes (W3). • B – width of occipital ring (W2) against maximum width of glabella (W1). • C – width across the eyes (W3) against width across the preocular genae (W7). • D – length of glabella (L1) against length of the palpebral lobe from point γ to point ε (L3).

that a specimen plotting to the left on the PC 1 axis has a proportionally narrow cranidium and large glabella, while a specimen plotting to the right has a broad cranidium and smaller glabella. Thus the shape of the glabella becomes more elongated and narrow in specimens towards the left on the PC 1 axis.

Specimens plotting high on the PC 2 axis have proportionally long glabella (L1) and long palpebral lobes (L3), and a narrow cranidium. Those plotting low on the axis have broad cranidia (W7) and are relatively broad across the eyes (W3).

PCA does not separate the relative differences between cranidia of *H. vikensis* and *H. spinulosus* very well, although specimens of *H. vikensis* tend to plot high on PC 2. The type cranidia of *H. vikensis* (NRM Ar 60130, NRM Ar 60131; Rushton & Weidner 2007, pl. 1, figs 11, 13) plot higher than the others, reflecting the proportionally narrow

cranidia. The largest specimen of *H. vikensis* (NHM It29261) plots low on the PC 2 axis, which reflects a proportionally broad cranidium with relatively short palpebral lobes and glabella. This is also evident in the bivariate plot (Fig. 8D), although the difference was not statistically significant.

Discussion. – The bivariate and PCA analyses give consistent results. The most variance occurs in the length of the cranidium and glabella relative to the greatest widths as specimens grow, which is consistent with results from similar studies and a common trait in trilobites (Esteve 2014 and references therein). The relative differences in variance are helpful to explain the components of allometric growth involved, but in this case it mostly did not contribute to the differentiation of the species analysed.
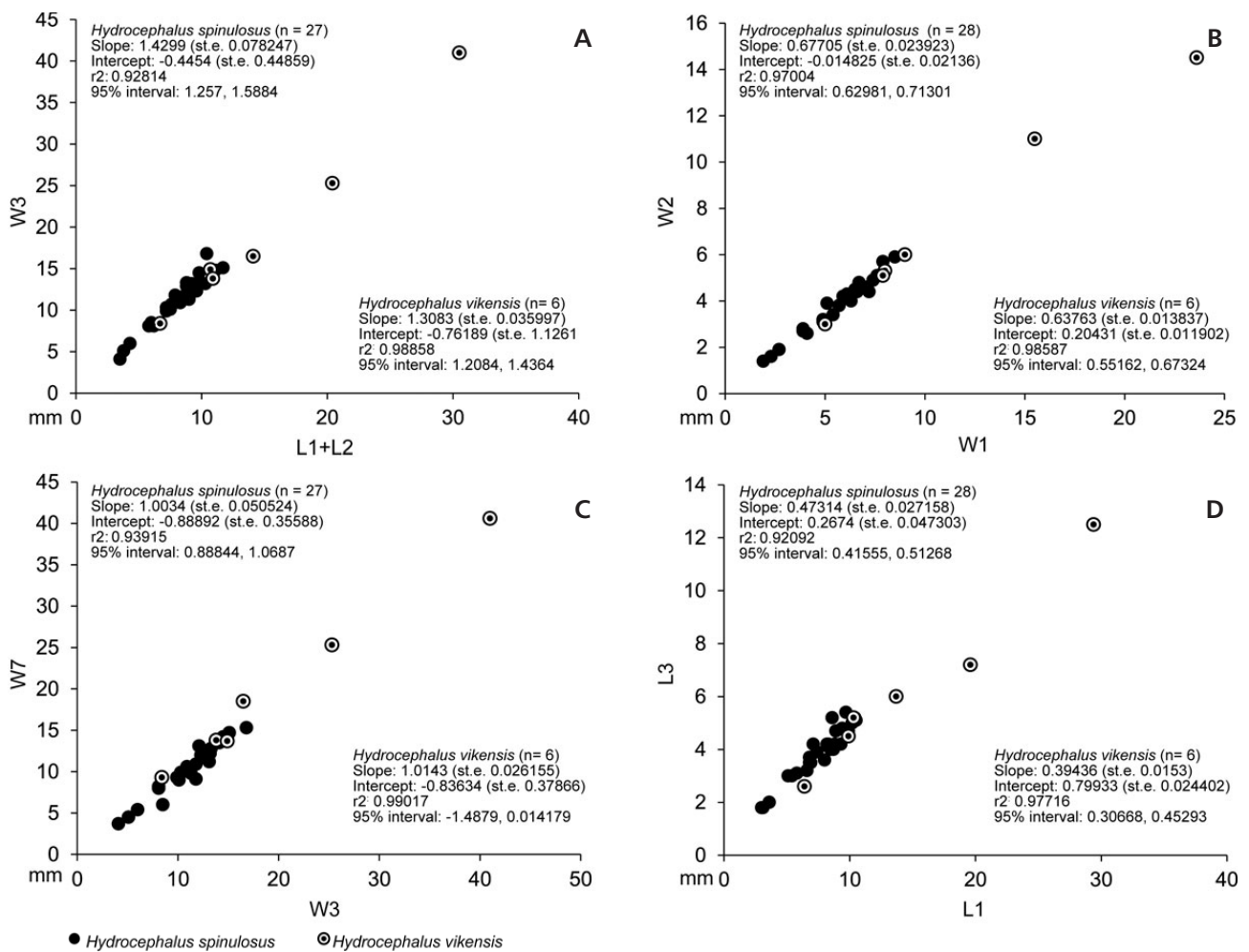
523

Figure 8. Bivariate plots and regression statistics of measurements made on cranidia of *Hydrocephalus spinulosus* and *H. vikensis*. The 95% confidence interval is given for the slope. St. e. = standard error. See Fig. 6 for further explanation of the measured parameters. • A – total length of cranidium (L1+L2) against width across the eyes (W3). • B – width of the occipital ring (W2) against maximum width of glabella (W1). • C – width across the eyes (W3) against width across the preocular genae (W7). • D – length of glabella (L1) against length of the palpebral lobe from point γ to point ε (L3).

Both analyses did distinguished *E. pusillus*, but also showed that the morphological variance in a juvenile specimen is similar to that of *E.? thorslundi* and *E. insularis*. If this is a consistent pattern it cannot be evaluated here because of the small sample size of taxa other than *E.? thorslundi* and *H. spinulosus* and the overall diminutive size of most specimens. Esteve (2014) argued that small samples sizes tend to exaggerate some differences between taxa, which may falsely lead to distinction of different species. This is not the case here. The size distribution of *H. spinulosus* and *H. vikensis* is similar to that of *E.? thorslundi* (Table 1) and the morphological variance covers an overall similar space (Fig. 9A, B). When larger specimens are included, such as those for *Eccaparadoxides*, the small and homogenous size and morphological variance of the cranidia on the principal surface becomes evident in the apparent clustering of the plots to the left in the diagram (Fig. 9A).

Although there is a tendency for specimens of *Hydrocephalus vikensis* to cluster high on the PC 2 axis, the overlap with *H. spinulosus* is too great to distinguish the two species, and shows instead a continuous variation in the measured parameters. However, the present analyses were made only on linear measurements of the cranidia, not taking into account curvature, profiles, relative placements of features etc. The unresolved PCA variances emphasize the importance of adding such cranidial characters as well as characters seen in the thoracic region (see comparison of *H. vikensis* and *H. spinulosus* under systematic palaeontology and Figs 29–31).

Systematic palaeontology

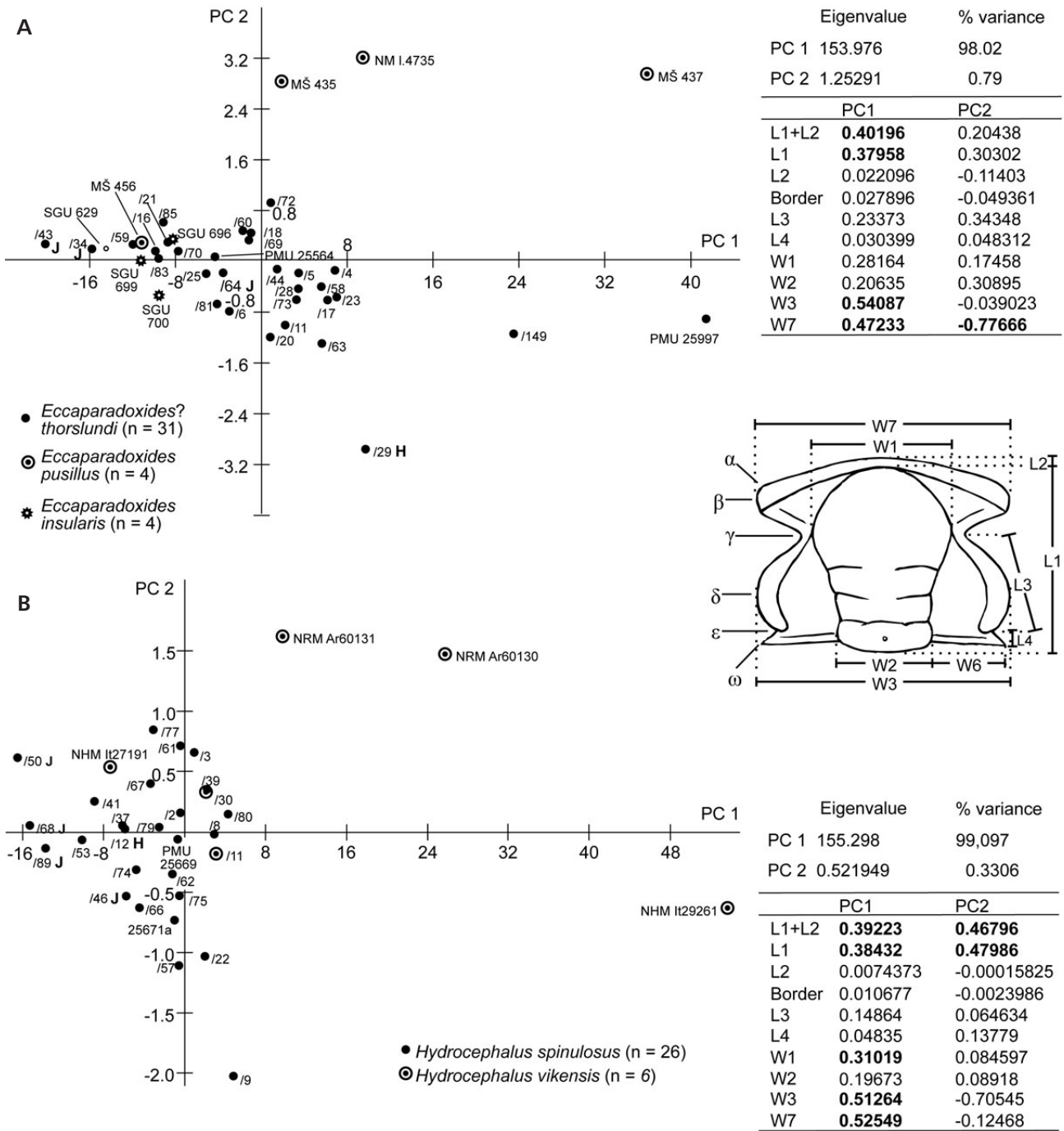The terminology used here is in Whittington & Kelly (1997), although we use "trunk" in place of "thoracopygon".

A

	Eigenvalue	% variance
PC 1	153.976	98.02
PC 2	1.25291	0.79

	PC1	PC2
L1+L2	**0.40196**	0.20438
L1	**0.37958**	0.30302
L2	0.022096	-0.11403
Border	0.027896	-0.049361
L3	0.23373	0.34348
L4	0.030399	0.048312
W1	0.28164	0.17458
W2	0.20635	0.30895
W3	**0.54087**	-0.039023
W7	**0.47233**	**-0.77666**

- • *Eccaparadoxides? thorslundi* (n = 31)
- ◉ *Eccaparadoxides pusillus* (n = 4)
- ✻ *Eccaparadoxides insularis* (n = 4)

B

	Eigenvalue	% variance
PC 1	155.298	99,097
PC 2	0.521949	0.3306

	PC1	PC2
L1+L2	**0.39223**	**0.46796**
L1	**0.38432**	**0.47986**
L2	0.0074373	-0.00015825
Border	0.010677	-0.0023986
L3	0.14864	0.064634
L4	0.04835	0.13779
W1	**0.31019**	0.084597
W2	0.19673	0.08918
W3	**0.51264**	-0.70545
W7	**0.52549**	-0.12468

- • *Hydrocephalus spinulosus* (n = 26)
- ◉ *Hydrocephalus vikensis* (n = 6)

Figure 9. Biplot of the first two principal components in the Principal Component Analysis (PCA) of eight measured parameters on paradoxidid cranidia. A slash followed by a number indicates a specimen from the principal surface and its sub-number (*e.g.* PMU 25711/No.). A bold **J** indicates juvenile specimens and a bold **H** indicates the holotype. • A – *Eccaparadoxides? thorslundi*, *E. pusillus* and *E. insularis* with PCA summary and loadings included. • B – *Hydrocephalus spinulosus* and *H. vikensis* with PCA summary and loadings included. The parameters measured are shown in the inset to aid the interpretation.

We use Greek letters to refer to particular points on the facial suture, as in Fig. 6 (*cf.* Weidner *et al.* 2014, fig. 9). "Lengths" generally refer to measurements in a sagittal direction and "widths" are generally transverse, and in ambiguous cases may be clarified by the abbreviations "sag." and "tr." The palpebral lobes are arcuate and are described as "broad" or "narrow", according to the separation in dorsal view of the palpebral furrow from the ocular suture. In recording measurements of the lengths of the thorax and pygidium, we exclude the articulating half-ring, because that feature is frequently not visible, being covered by the sclerite immediately in front.

Table 5. Measurements on cranidia of *H. spinulosus*. See Fig. 6 for explanations of the parameters. A '**J**' following the specimen number indicates a juvenile specimen.

Specimen	L1+L2	L1	L2	Border	PGF	L3	L4	W1	W2	W3	W6	W7
PMU 25669	9.5	8.9	0.6	0.6	–	4.7	0.8	7.1	4.6	13.1	4.5	11.2
PMU 25671a	8.8	8.3	0.5	0.5	–	4.2	1.0	6.5	4.4	12.9	4.2	12.2
PMU 25711/2	9.2	8.6	0.6	0.6	–	5.2	0.9	6.7	4.8	12.1	3.3	13.1
PMU 25711/3	10.3	9.7	0.6	0.6	–	5.4	1.0	7.7	5.1	13.2	3.8	12.3
PMU 25711/8	11.1	10.4	0.7	0.7	–	5.2	0.9	7.4	4.9	14.8	5.0	13.7
PMU 25711/9	10.4	9.9	0.5	0.5	–	4.7	1.0	8.5	5.9	16.8	3.8	15.3
PMU 25711/12 **H**	7.2	6.8	0.4	0.4	–	3.5	0.9	5.4	3.4	9.9	2.2	9.3
PMU 25711/22	9.8	9.3	0.5	0.5	–	4.2	1.1	7.4	4.9	14.5	–	14.2
PMU 25711/37	7.5	6.8	0.7	0.8	–	3.7	1.1	4.9	3.1	10.1	3.1	9.0
PMU 25711/39	10.9	10.2	0.7	0.7	–	5.0	1.0	7.6	5.1	14.1	–	13.5
PMU 25711/41	6.2	5.8	0.4	0.4	–	3.1	0.4	4.1	2.6	8.1	–	8.0
PMU 25711/46	7.2	6.6	0.6	0.4	0.2	3.2	0.6	4.9	3.2	10.3	2.5	9.9
PMU 25711/50 **J**	3.5	3.0	0.5	0.3	0.2	1.8	0.3	1.9	1.4	4.1	–	3.7
PMU 25711/53	6.0	5.4	0.6	0.5	0.1	3.0	0.5	3.9	2.7	8.5	–	6.0
PMU 25711/57	8.8	8.3	0.5	0.5	–	4.1	0.8	6.5	4.5	13.3	–	12.8
PMU 25711/61	9.6	9.4	0.2	0.2	–	4.8	0.9	7.2	4.4	12.3	–	12.0
PMU 25711/62	9.3	8.7	0.6	0.7	–	4.0	0.9	6.1	4.3	13.0	4.8	11.4
PMU 25711/65	–	7.1	–	–	–	4.2	0.7	5.9	4.2	12.1	3.5	–
PMU 25711/66	7.9	7.4	0.5	0.5	–	3.9	0.8	5.1	3.9	11.8	–	9.1
PMU 25711/67	8.3	8.0	0.3	0.3	–	3.6	0.9	6.3	4.0	10.9	2.5	10.6
PMU 25711/68 **J**	3.8	3.1	0.7	0.3	–	1.8	0.3	2.3	1.6	5.1	1.4	4.5
PMU 25711/74	7.6	6.9	0.7	0.8	–	3.5	1.0	5.7	3.8	10.7	3.3	10.1
PMU 25711/75	9.2	8.8	0.4	0.4	–	4.2	0.9	6.6	4.4	13.2	4.4	12.2
PMU 25711/77	9.0	8.5	0.5	0.5	–	4.0	1.1	6.1	4.3	11.3	–	9.8
PMU 25711/79	8.7	8.2	0.5	0.6	–	4.2	0.8	6.2	4.1	11.8	–	10.9
PMU 25711/80	11.7	10.5	1.2	1.2	–	5.1	1.3	7.9	5.7	15.1	4.5	14.7
PMU 25711/89 **J**	4.3	3.6	0.7	0.3	0.4	2.0	0.4	2.7	1.9	6.0	–	5.4
PMU 25711/91	5.8	5.1	0.7	0.7	–	3.0	0.5	3.9	2.8	8.1	1.9	8.2

Table 6. Measurements on cranidia of *H. vikensis*. See Fig. 6 for explanations of the parameters.

Specimen	L1+L2	L1	L2	Border	PGF	L3	L4	W1	W2	W3	W6	W7
25711/11	10.7	10.3	0.4	0.4	–	5.2	1.2	8.0	5.3	14.9	3.7	13.7
25711/30	10.9	9.9	1.0	1.0	–	4.5	0.8	7.9	5.1	13.8	4.3	13.8
NRM Ar60130a-b	20.4	19.6	0.6	0.6	–	7.2	2.6	15.5	11.0	25.3	8.5	25.3
NRM Ar60131	14.1	13.7	0.7	0.7	–	6.0	2.0	9.0	6.0	16.5	~4.5	~18.5
NHM It29216	30.5	29.4	1.1	1.1	–	12.5	3.5	23.6	14.5	41.0	13.5	40.6

Except where otherwise indicated, all the figured specimens are from the "Big Block". Individual specimens on the principal surface of the "Big Block" (PMU 25711) were given sub-numbers in Ebbestad *et al.* (2013, fig. 2), which are used here.

Nearly all of the fossils discussed here are housed in the Museum of Evolution, Uppsala, Sweden, with registered numbers having the prefix PMU. A few specimens are from the Swedish Museum of Natural History, Stockholm (NRM), the Swedish Geological Survey, Uppsala (SGU), the Národní muzeum, Prague (NM), and in the Natural History Museum, London (NHMUK).

Family Paradoxididae Hawle & Corda, 1847

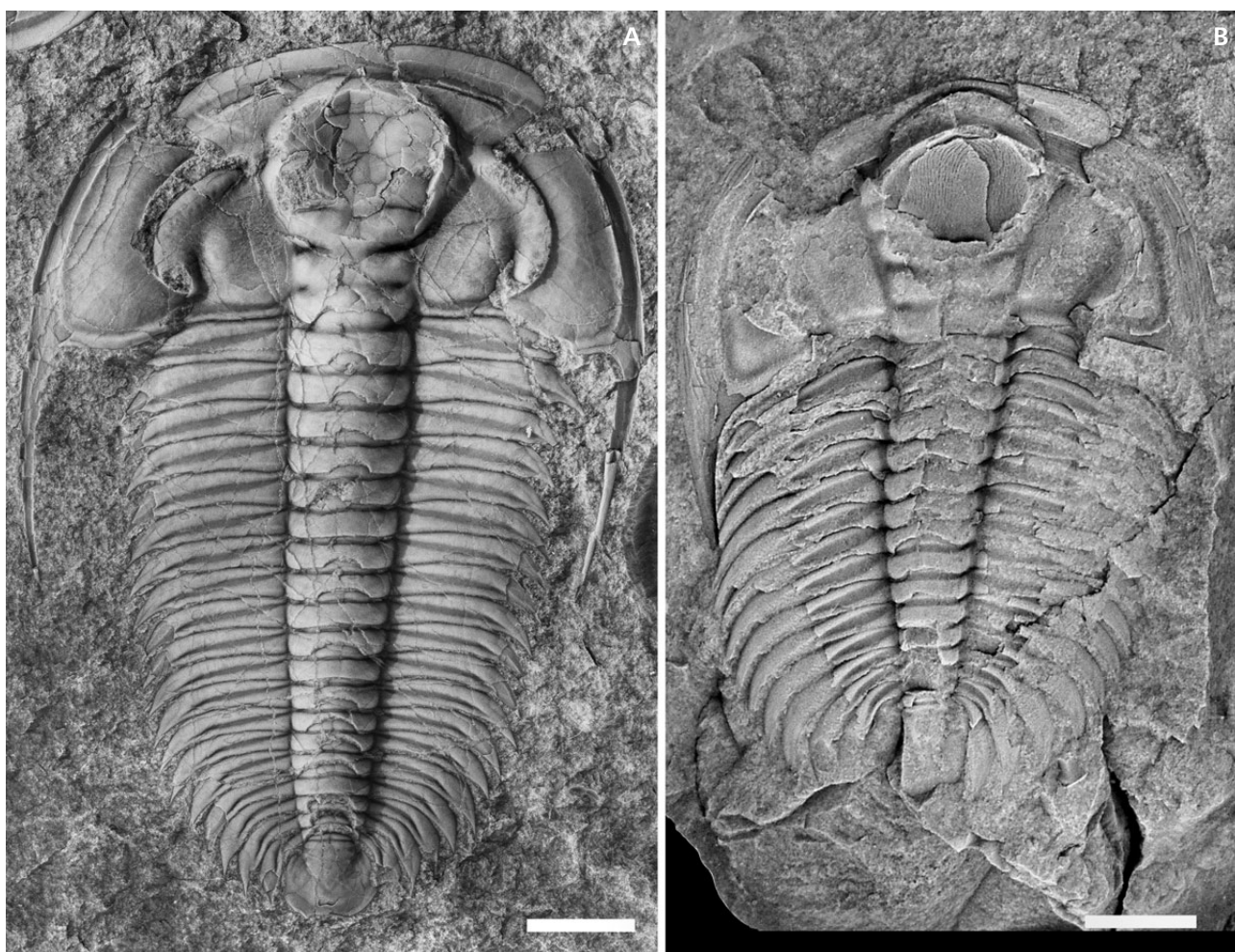We follow the generic arrangement given by Dean & Rushton (1997), despite the unresolved problems mentioned by

Figure 10. A – *Eccaparadoxides*? *thorslundi* sp. nov. PMU 25711/29, holotype. • B – *Eccaparadoxides pusillus* (Barrande), Czech Geological Survey, Prague, ČGÚ VK28 from the Jince Formation at Rejkovice, Prague Basin. Scale bars = 5 mm.

Geyer & Landing (2000) and Fletcher *et al.* (2005), because their listing remains fairly complete.

Genus *Eccaparadoxides* Šnajdr, 1957

Type species. – *Paradoxides pusillus* Barrande, 1846, by original designation.

Description. – The lectotype of *E. pusillus* is a meraspid with a sagittal length of 2 mm, the cephalon being just over 1 mm long (Šnajdr 1958, pl. 20, fig. 43). It is from the Buchava Formation at the locality Pod hruškou, Týřovice, Czech Republic, whence a great number of additional specimens have been obtained that have enabled a reconstruction of the ontogeny (Šuf 1926; Šnajdr 1958, pls 20–22; text-figs 20, 21). Well-grown specimens may have cephala more than 25 mm long.

Remarks. – Geyer & Vincent (2014, p. 23) have remarked that the widely used genera *Acadoparadoxides* and

Eccaparadoxides proposed by Šnajdr (1957, 1958) have type species that are not ideally representative of the generic groups they are assigned to. However, we consider that several species commonly assigned to *Eccaparadoxides*, for example *E. pusillus*, *E. insularis*, *E. pradoanus*, *E. rouvillei*, *E. acadicus* and *E. eteminicus*, form a usable morphological group that includes species known from Bohemia, Sweden, the Mediterranean area and Avalonian parts of North America. These species of *Eccaparadoxides* appear to represent a crown group of uncertain ancestry, and its antecedents may lie in an unresolved paraphyletic group that includes, or may be related to, *Anabaraspis* species from the Siberian Platform.

***Eccaparadoxides*? *thorslundi* sp. nov.**
Figures 10A, 11A–H, 12–19

> 2007 *Acadoparadoxide*s (*Baltoparadoxides*) sp. nov.; Münder, p. 145, fig. 3.
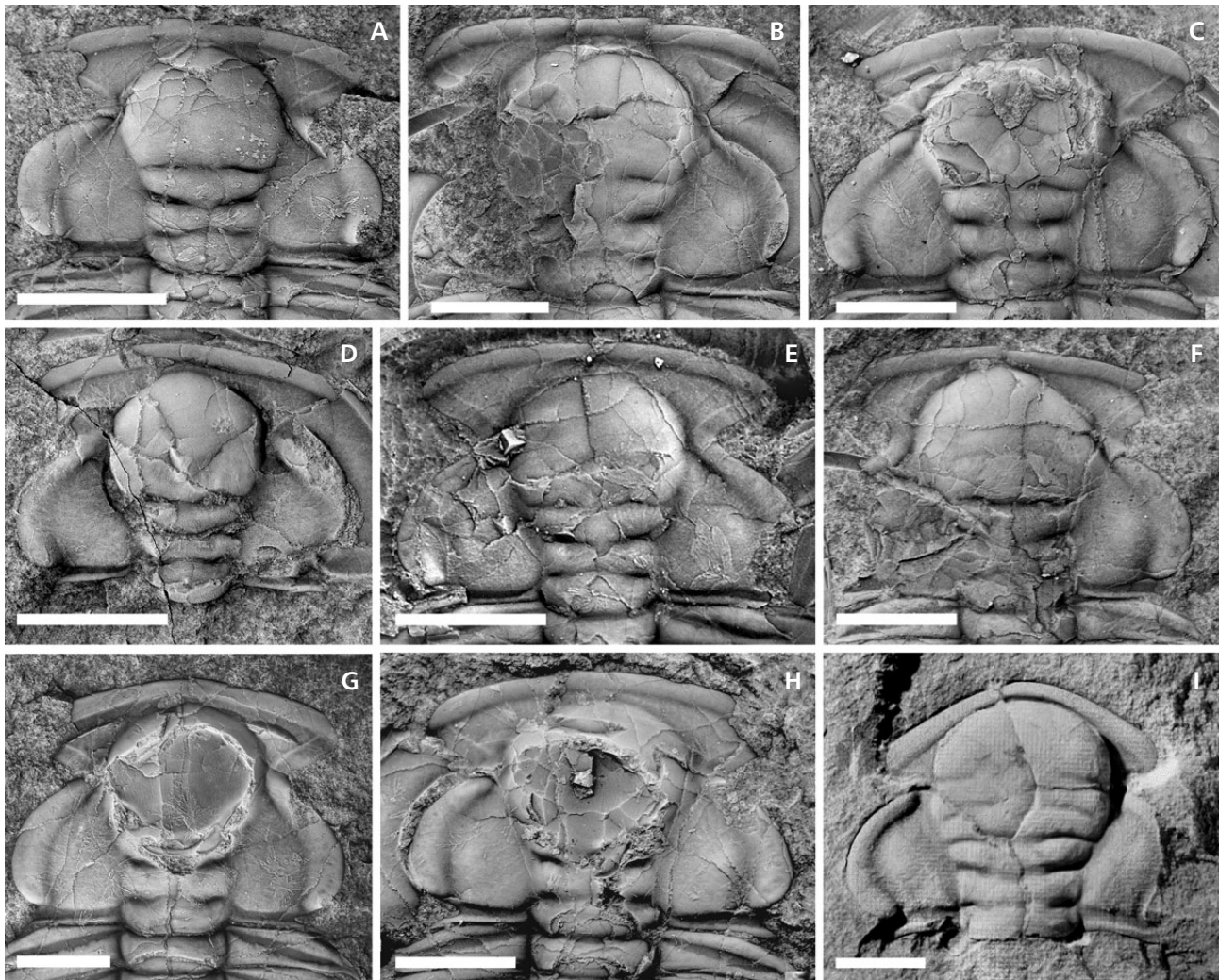
Figure 11. A–H – *Eccaparadoxides*? *thorslundi* sp. nov., cranidia. • A – PMU 25711/25, small but typical, with narrow preglabellar field; shows granulated surface and lack of S3 and S4. • B – PMU 25711/28, note glabellar furrows and narrow preglabellar field. • C – PMU 25711/1, shows occipital node, facial line and caeca on interocular genae. • D – PMU 25711/42, note occipital node. LO, L1 and L2 have a finely granulated surface. • E – PMU 25711/6 shows both facial lines. • F – PMU 25711/44, preglabellar furrow and border furrow merged. • G – PMU 25711/17, preglabellar furrow and border furrow merged, caeca on interocular genae. • H – PMU 25711/20, caeca on preocular and interocular genae. • I – *Eccaparadoxides pusillus* (Barrande), NM Prague, I.4735, topotype. Scale bars = 5 mm.

2013 *Eccaparadoxides* sp. 2; Ebbestad *et al.*, p. 20, figs 3D, E, 6A, C, 9A–C.

Holotype. – PMU 25711/29 (Fig. 10A), a moulted exoskeleton 41 mm long on the principal surface of the "Big Block". It shows all parts of the dorsal shield.

Material. – 46 articulated exoskeletons, many small and fairly complete, from the "Big Block" (PMU 25711), collected at Tännberget quarry, Östnår, Jämtland (Ebbestad *et al.* 2013); also several other fragments from Östnår, Travbanan (Hackås), Mon and Brunflo, and an axial shield from Klocksåsen, 14 km SW of Brunflo.

Etymology. – Named after Professor Per Thorslund, Upp-sala, in recognition of his contributions to the geological understanding of Jämtland and Ångermanland in Sweden.

Diagnosis. – A species of *Eccaparadoxides*? with a comparatively narrow cephalic border and slender genal spines; glabellar furrows S3 and S4 indistinct or not well developed in holaspids; palpebral lobes broad, especially posteriorly; thorax with 19 segments, the anterior 10–11 segments transverse, the pleurae of all segments having the pleural furrows extending almost to the pleural tips; all the pleural spines short; pygidium subhexagonal, wider than long, the posterior margin weakly embayed with a pair of obtuse points; pygidial axis rather indistinctly segmented, about two-thirds of pygidial length, commonly with a post-axial swelling.
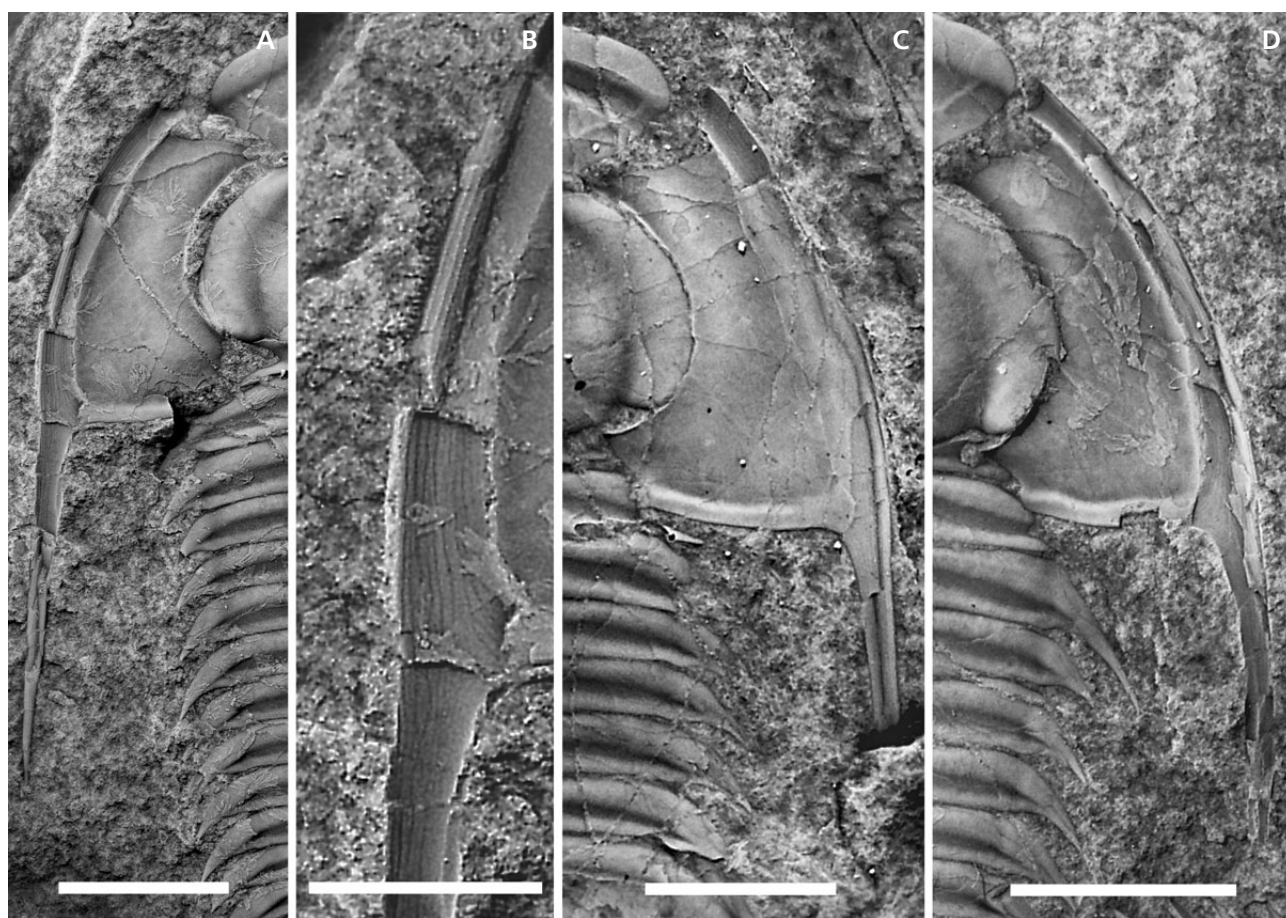
Figure 12. *Eccaparadoxides*? *thorslundi* sp. nov., librigenae. • A, B – PMU 25711/20. Where the doublure has broken away, the external mould shows the ventral terrace-lines. • C – PMU 25711/63. • D – PMU 25711/1. Scale bars = 5 mm, except in Fig. 12B where it is 2.5 mm.
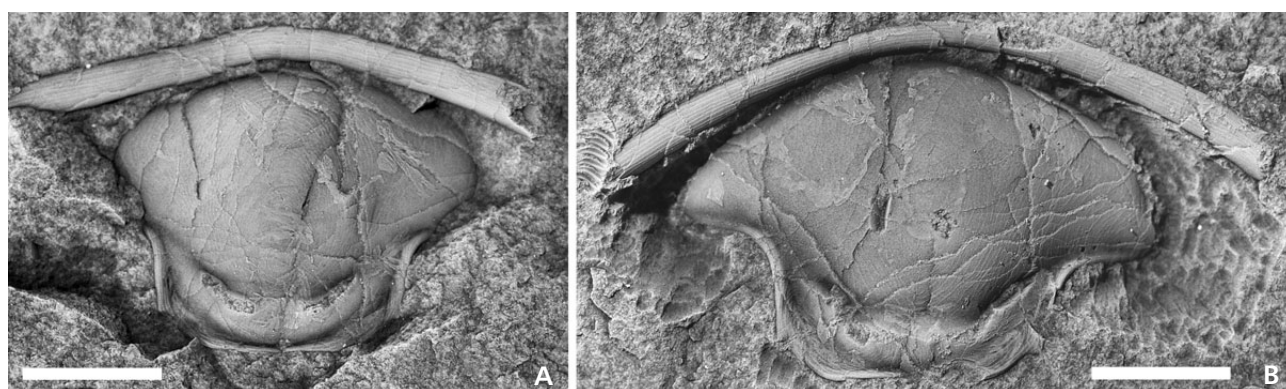
Figure 13. *Eccaparadoxides*? *thorslundi* sp. nov., hypostomata. • A – PMU 25711/14. • B – PMU 25711/45. Scale bars = 5 mm.

Description. – Dorsal exoskeleton (including librigenae) has a maximum width about 2/3 of its length. Cephalon semi-circular (excluding the genal spines), length about 1/3 of the length of the exoskeleton. Maximum width of thorax about half of the exoskeletal length and the pygidium less than one tenth of the exoskeletal length.

Glabellar outline has concave sides and is well rounded in front (Fig. 11A, G). The posterior part (LO and L1) is nearly parallel-sided; but anterior of S1 it widens forwards strongly, commonly attaining a width about 1.4 times that of LO (average 1.37 see Fig. 7B). Where the occipital ring is well preserved, a small median node is commonly visible (Fig. 11A, C, D), but in some specimens it cannot be discerned. SO is transglabellar; deep laterally but becomes

529
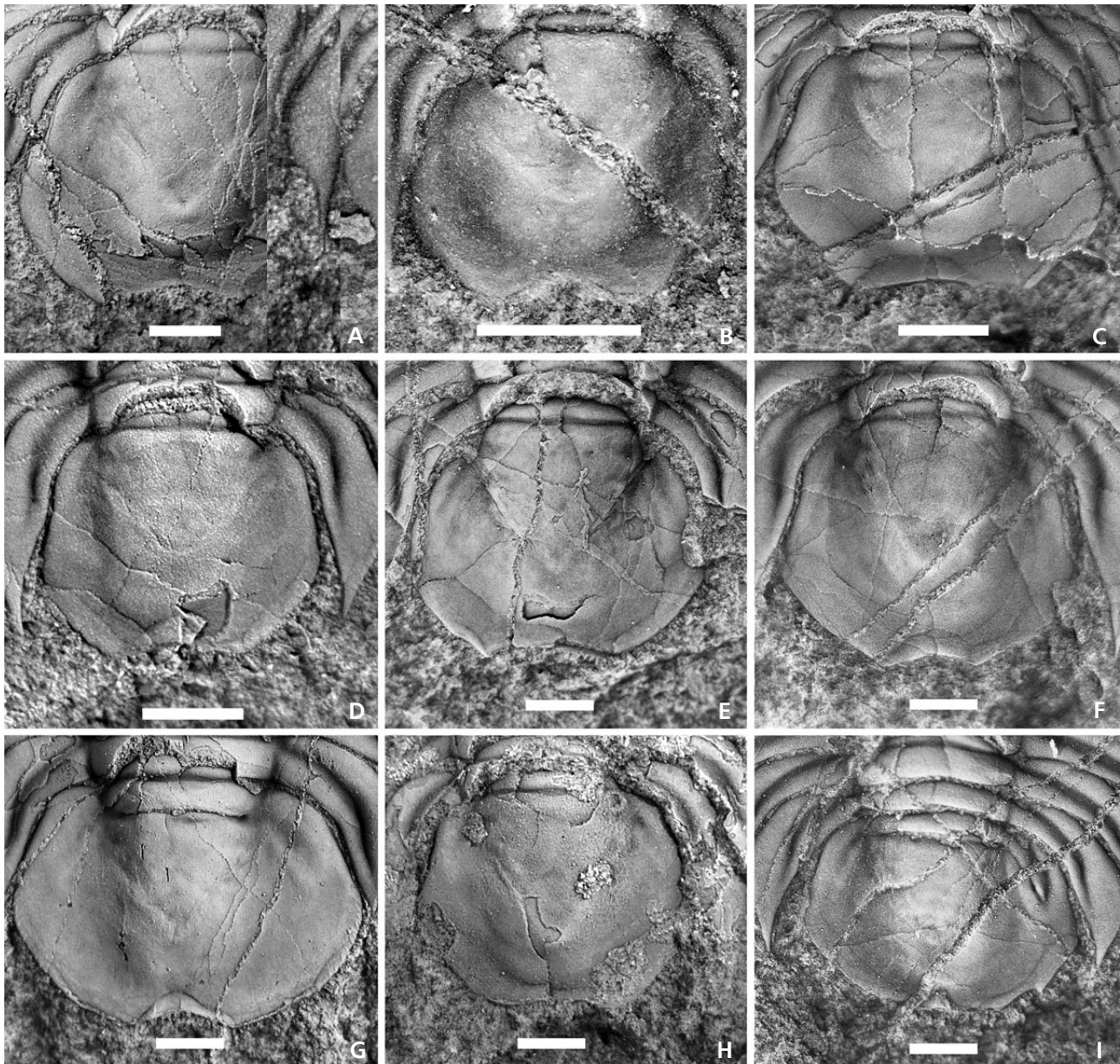
Figure 14. *Eccaparadoxides*? *thorslundi* sp. nov., pygidia. • A – PMU 25711/24, part of doublure is shown posteriorly. • B – PMU 25711/16, pronounced posterior indentation. • C – PMU 25711/72, with cusps that delimit a wide indentation. • D – PMU 25711/64. • E – PMU 25711/29 (holotype); axis conical, marginal spine on left side. • F – PMU 25711/58, with weak post-axial swelling or "platform". • G – PMU 25678 from Östnår (see Fig. 19B, aberrant transverse form). • H – PMU 25648, locality Travbanan; shows postaxial swelling. • I – PMU 25711/18 showing an anomalous pleural structure on right side. Scale bars = 1 mm.
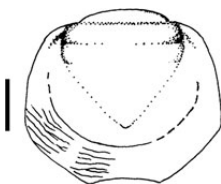
Figure 15. *Eccaparadoxides*? *thorslundi* sp. nov. A reconstruction to show the extension of the doublure of the pygidium, based on fragmentary information. Scale bar = 1 mm.

shallow medially where it is slightly bowed forward. L1 is no wider (tr.) than LO and may even be a little less wide. Lateral parts of S1 deep and connected with the axial furrow; adaxially they are directed transversely or slightly obliquely backwards, and rapidly become shallow (Fig. 11B, C); they may fade out before reaching the sagittal line or may connect weakly across the glabella. L2 widens forward. S2 furrows narrower than S1 and nearly transverse; they do not connect distinctly with the axial furrow, nor connect strongly across the glabella. In one or two specimens, S3 is seen inclined inwards and forwards, but it is very faint (Fig. 11F); S4 is effaced in holaspid specimens (Fig. 11A, D, E).
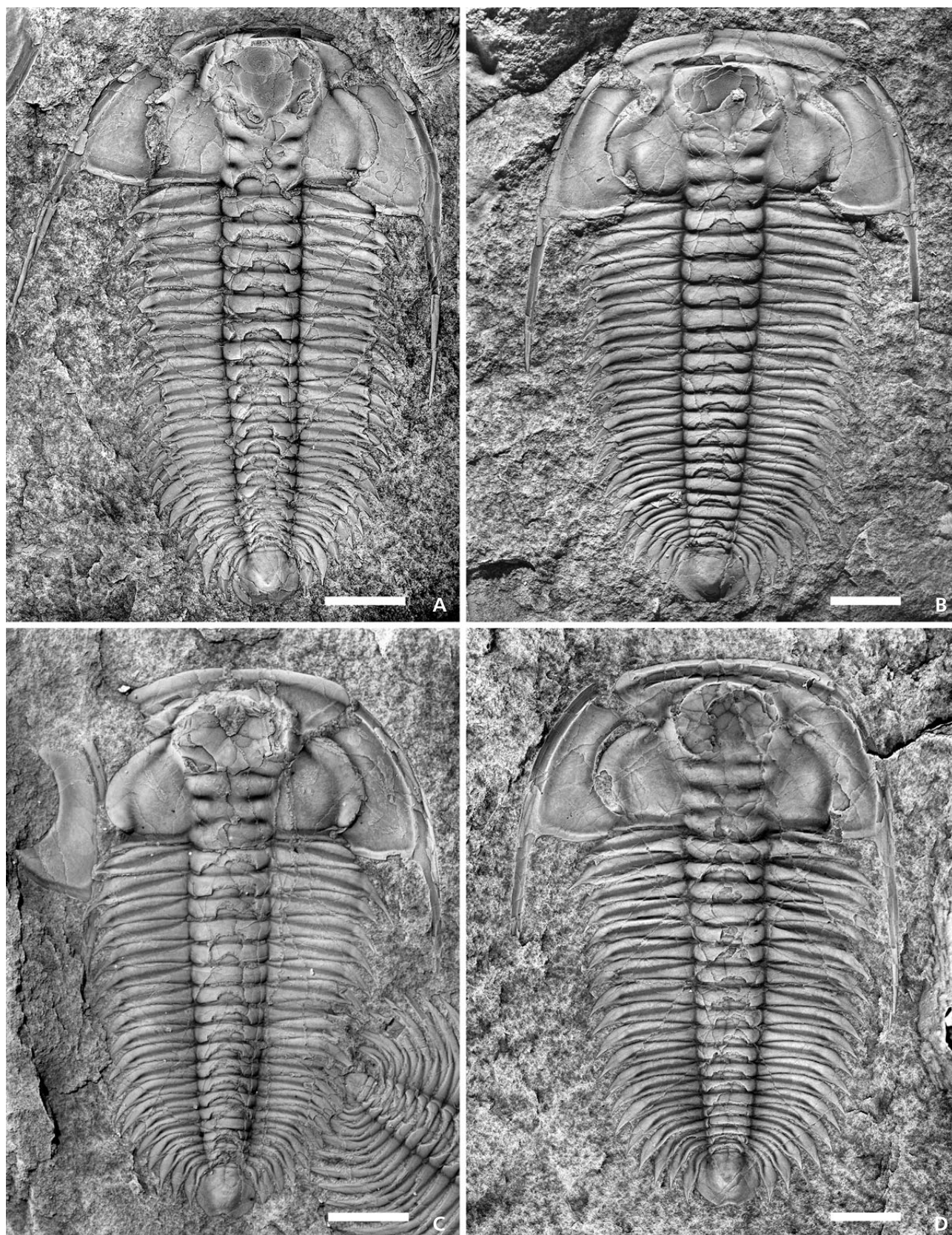
Figure 16. *Eccaparadoxides*? *thorslundi* sp. nov., axial shields. • A – PMU 25711/24. • B – PMU 25711/23. • C – PMU 25711/1. Moulted left librigena is inverted. • D – PMU 25711/58, rubber cast. Scale bars = 5 mm.

Frontal border distinct, slightly convex longitudinally, rather narrow (< one-tenth of cranidial length) and of fairly even width (sag., exsag.), particularly in the small holaspids on the principal surface; but it may be slightly wider (exsag.) near point α, especially in larger specimens (Fig. 18F). The glabella generally extends forward almost to the anterior border furrow; it does not encroach on the border, and the preglabellar furrow may merge with the anterior border furrow (Fig. 11F, G); but in many cranidia it falls short, leaving a narrow preglabellar field that is commonly about half or one-third as wide (measured longitudinally) as the border at the mid-line (Fig. 11E, G, H). The frontal area is about one tenth of the glabellar length but in a meraspid specimen with a cephalic length of 5 mm, the frontal area is proportionately more than twice as long sagittally (Fig. 17C). Transverse width of preocular fixigenae (β–β) about nine-tenths of the width across the palpebral lobes (δ–δ). The preocular facial line is generally seen parallel to the suture between points β and γ (Fig. 11C, E). Point γ lies close to the widest part of the glabella, and is separated from it by a fixigenal strip that is commonly about 0.15 to 0.2 of the maximum width of the glabellar. Palpebral lobe oblique, arcuate and turned inwards posteriorly, extending from near the widest part of the glabella and ending just above the posterior border furrow; the lobe is broader and more strongly curved in its posterior half; its exsagittal length (points γ to ε) is 0.6 of the glabellar length (Fig. 7D). Width of cranidium across the palpebral lobes (δ–δ) is three times the width of LO. The postocular suture (ε–ω) is very short. The surface of the glabella generally appears smooth, but when favourably preserved the exoskeleton may show a fine and subdued granulation: the granules are about 0.05 mm in diameter and lie about 0.1 mm apart (comparable to the thoracic segment shown in Fig. 19E). In a few specimens the interocular genae and frontal area show faintly the genal caeca as a network of raised ridges (Fig. 11C, G, H).

The librigena (Fig. 12) has a rather broad genal field that is more than twice as wide as the border, which is narrow. The genal spine is correspondingly slender and extends back about as far as the eighth thoracic segment. The posterior margin of the librigena is gently curved, convex backwards, and the inner spine angle is a little more than 90 degrees. A few librigenae show genal caeca: the genal ridge (or "principal genal vein" of Öpik 1967, p. 215) extends from near point δ towards the genal angle (Fig. 12D).

A number of hypostomata and rostra that are associated with exuviae (Ebbestad *et al.* 2013, fig. 9) do not show clearly details of their morphology. Separate hypostomes that are detached from exuviae are less securely assigned to a particular species. Hypostomes that we refer to *E.? thorslundi* (Fig. 13A, 13 mm wide and 10 mm long; Fig. 13B, 17 mm wide and 11.4 mm long) were cast by animals with larger cranidia than any seen on the principal surface of the "Big Block". They are transverse, with sagittal length about two-thirds of the maximum width. The posterior border is transverse medially; abaxially it trends obliquely outwards and forwards to a very short marginal spine; beyond this the margin become almost exsagittal before turning outwards to become nearly transverse. The posterior lobe of the middle body of the hypostome is also transverse, and the maculae are extended. The middle body of the hypostome has terrace lines forming a longitudinally oval whorl (Fig. 13A). Rostra associated with these hypostomes are 1.3 times wider than the hypostome and their median length (sag.) is slightly less than that of the posterior lobe of the middle body (Fig. 13B).

Thorax of 19 segments in the holaspid, seen in at least 20 dorsal and axial shields ranging in length from 20 mm to 70 mm; we have not seen any specimen with more than 19 free segments (but see below for a note on the anomalous specimen in Fig. 19C). The anterior pleurae are transverse and end in short spines (Fig. 19B), though in several specimens the spines on the second segment are very slightly elongated (Fig. 16A, C, D). Pleural grooves long (tr.), extending to the bases of the pleural spines. The more posterior segments, from about the eleventh, become narrower (tr.) and more arcuate and the last segment curves neatly round the sides of the pygidium. No pleura extends farther back than the posterior edge of the pygidium (Figs 16, 19). The pleural doublure is not well seen, but appears (Figs 14A, 15) to extend less far towards the axial furrow than that of *Eccaparadoxides pusillus* (Šnajdr 1958, pl. 22, figs 3, 4) or *E. eteminicus* (Kim *et al.* 2002, fig. 7). The thoracic segments may show a fine granulation (Fig. 19D, E), similar to that on the cranidium.

Pygidial outline somewhat variable, generally wider than long by about 4:3, more or less hexagonal, widening backwards to reach a maximum at about two-thirds of the sagittal length, behind which it narrows to the posterior margin; this may be nearly transverse but with a median indentation that is generally shallow (Fig. 14C, H), but may be more pronounced, as in Fig. 14B, F. Some specimens show cusps that delimit the indentation (Fig. 14C) or there may be tiny spines, sometimes asymmetrically disposed (Fig. 14E, I). The pygidial axis is conical (Figs 14A, 18E)

Figure 17. *Eccaparadoxides*? *thorslundi* sp. nov., juvenile specimens. • A – PMU 25711/43, a moult with librigena inverted laterally. • B – PMU 25711/38. • C – PMU 25711/34. • D – PMU 25711/21, a small holaspid. Scale bars = 5 mm.
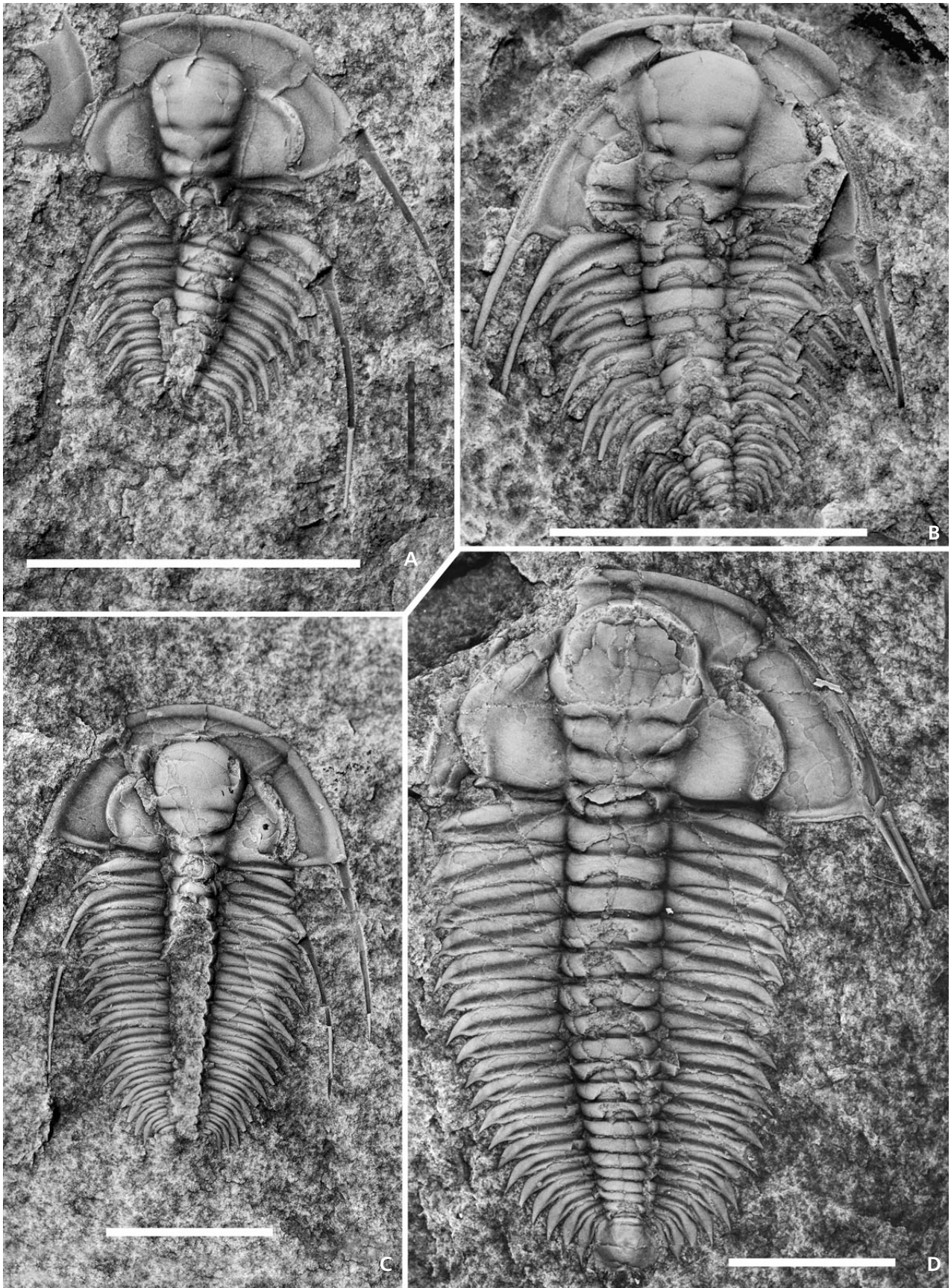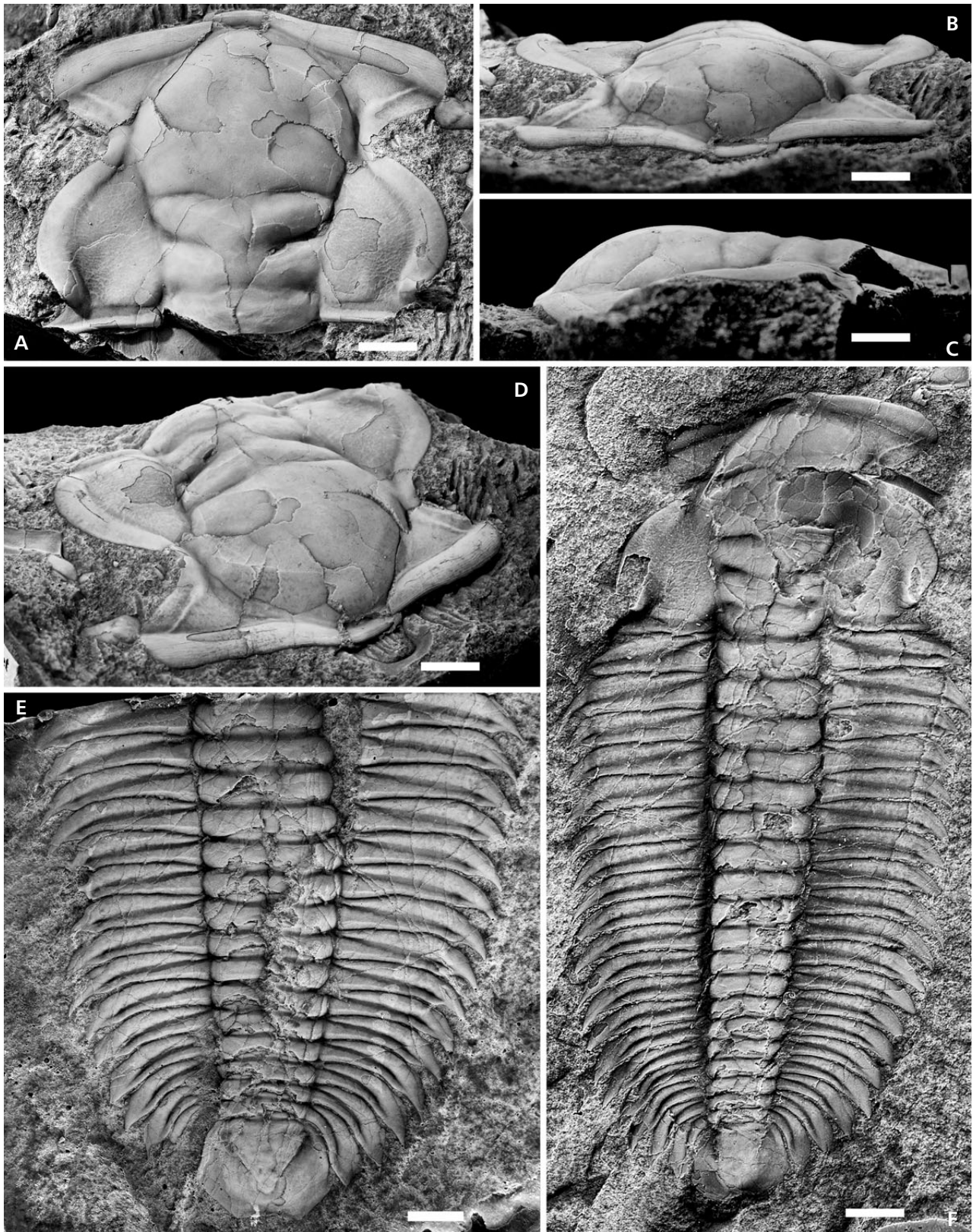
Figure 18. *Eccaparadoxides*? *thorslundi* sp. nov. • A–D – PMU 25997, locality Brunflo. A cranidium, slightly crushed, tentatively assigned to this species; dorsal, anterior, left lateral and dorsal oblique views respectively. • E – PMU 25711/55, large fragment of thorax with pygidium. Latex cast. • F – PMU 25711/149, large axial shield, showing the trace of a backwardly-displaced rostrum. Latex cast. Scale bars = 5 mm.
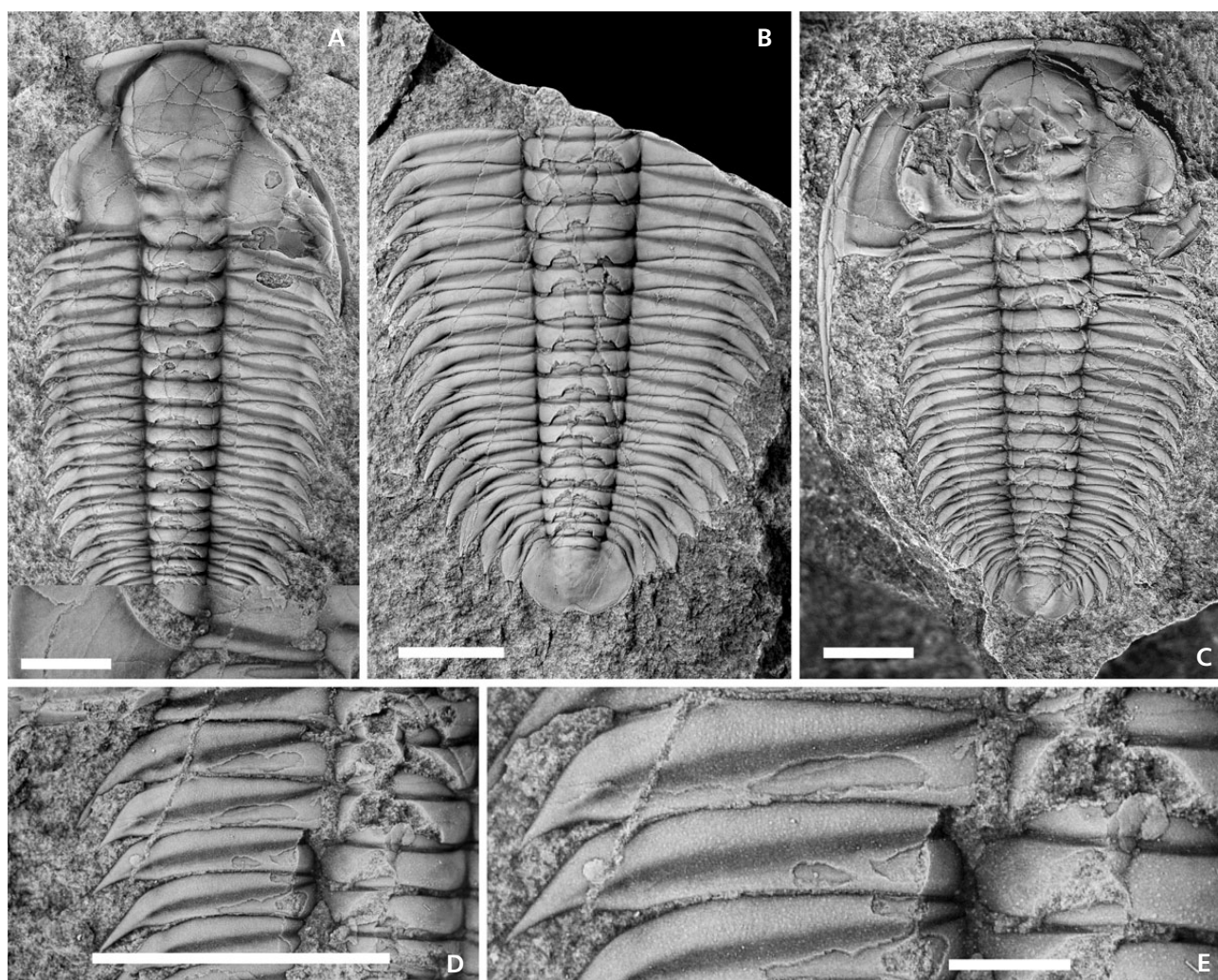
Figure 19. *Eccaparadoxides*? *thorslundi* sp. nov. • A – PMU 25711/72. Latex cast. • B – PMU 25678, Östnår. The pygidium is abnormally transverse. • C – PMU 25711/18, with pathological pygidium (see Fig. 14I). • D, E – PMU 25711/16. • D – part of thorax showing the longer spine on the second segment (macrospine), and E – detail of segments showing granulate sculpture. Scale bars for A–D = 5 mm, for E = 1 mm.

with a maximum width 0.5 to 0.65 that of the maximum pygidial width. Commonly segmentation of the axis is obscure (Fig. 14F). In some specimens one axial ring is faintly seen or rarely is distinct (Fig. 14G) and there may be a trace of a second one. The posterior part of the axis generally merges with a weak post-axial swelling or "platform" of Geyer & Vincent (2015, *e.g.* figs 16, 21); the axial furrow becomes shallow and faint on the swelling, but the tip of the axis is commonly recognisable and indicates that the axis tapers from the articulating furrow back to a point about 0.6 to 0.7 of the pygidial length (Fig. 14A, H). The pleural fields usually show a trace of a pleural furrow proximally. The pygidial doublure is not well known, but parts of it are seen in broken specimens. It appears to extend forward from the posterior margin by about one-quarter of the pygidial length (Fig. 14A, D); six or seven terrace lines can be seen in places, as reconstructed in Fig. 15).

Figure 14I shows a malformed pygidium comparable with those sometimes seen in paradoxidids, wherein the posterior thoracic segment is partly fused to the pygidium on one side (*cf.* Westergård 1936, pl. 8, fig. 4, pl. 10; Šnajdr 1958, pl. 42, figs 8, 9; Rushton & Weidner 2007, pl. 3, fig. 17). The present exoskeleton has 19 free thoracic segments, the normal holaspid number for this species (Fig. 19C), and the anomalous pleura on the right side of the pygidium appears to represent an abortive 20th segment; the pygidial margin on the left side lacks spines but the right side shows two small marginal spines.

Juvenile specimens. – The exuviae of immature specimens on the principal surface are not very complete, but a few of them can be assigned to *E*? *thorslundi* (see Table 7).
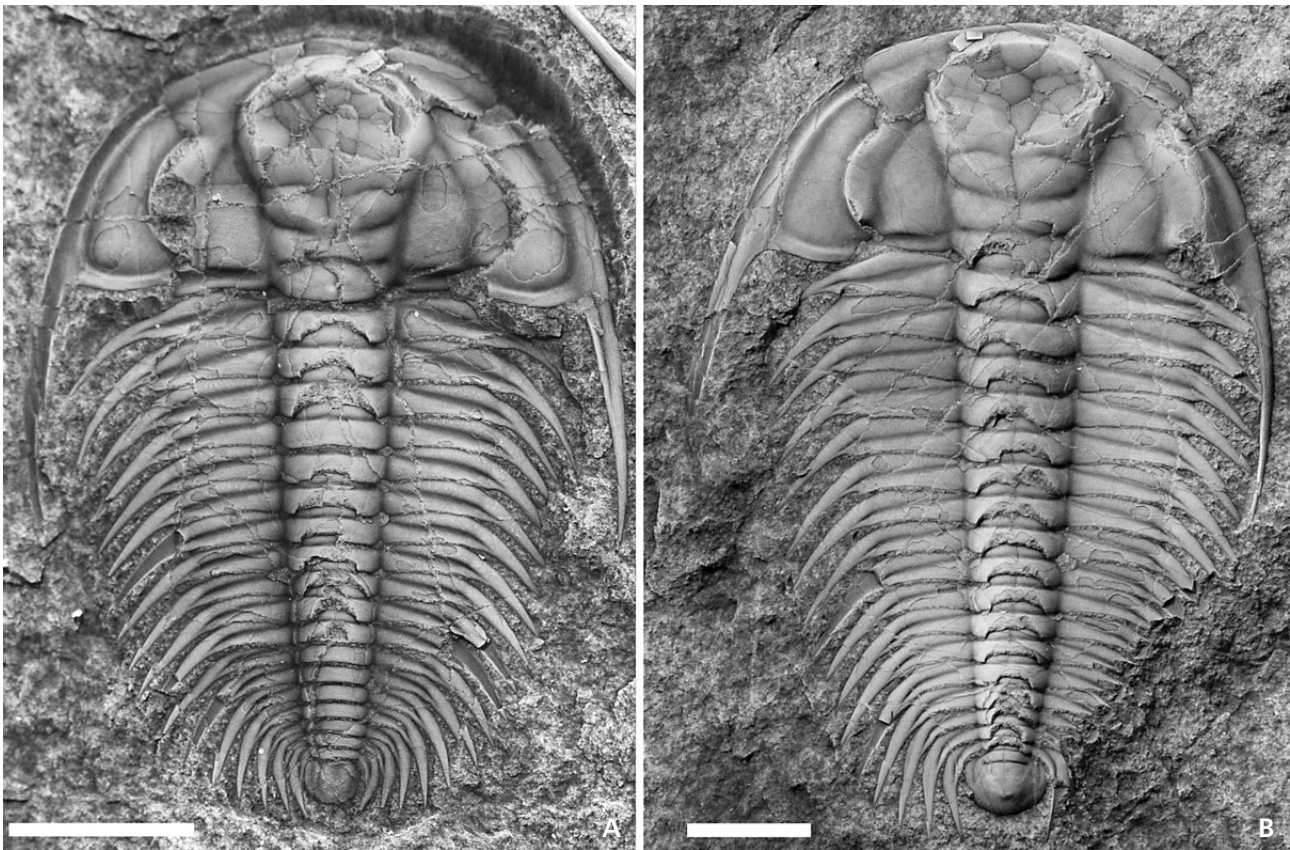
535

Figure 20. A – *Hydrocephalus spinulosus* sp. nov. PMU 25711/12, holotype. • B – *Hydrocephalus vikensis*, PMU 25711/11. Scale bars = 5 mm.

Table 7. Juvenile specimens of *Eccaparadoxides*? *thorslundi* on the principal surface of the Big Block.

Fig.	Cranidial length (mm)	Remarks
17A	2.9	9 or 10 free segments seen. Anterior segment fragmentary and pygidium not seen. Macrospines on 2nd segment. Preglabellar field 20% of cranidial length. S3 and S4 shallow but distinct.
17B	3.1	15 free segments. Anterior segment fragmentary and pygidium not clear. Macrospines on 2nd segment. Preglabellar field 16% of cranidial length. S3 and S4 scarcely visible.
17C	5.2	17 segments at least, no pygidium. 2nd segment retains long pleural spines. Preglabellar field 12% of cranidial length. S3 and S4 not seen.
17D	7.6	Small holaspid (19 free segments). Spine on 2nd pleura of normal length. Preglabellar field is *ca* 4% of glabellar length.

Measurements. – The holotype (Fig. 10A) has a sagittal length of 41 mm and the width of the thorax is 22 mm; the cranidial length is 13.8 mm and pygidial length 3.5 mm. Specimen PMU 25711/76 (the external mould on Fig. 5, to the right, half way down), the largest complete axial shield on the principal surface, is 58 mm long. A larger axial shield (Fig. 18F), which was found on the underside of the "Big Block", is 69 mm long; the cranidium as preserved is 20.5 mm long and 25.9 mm wide across the palpebral lobes (δ–δ). An incomplete trunk on the principal surface (Fig. 18E) represents a specimen twice the size of the holotype. Judging from the width of this thorax, it seems that the whole exoskeleton may have been nearly 90 mm long. The pygidium is 8.8 mm long and 12.5 mm wide. A large cranidium from Brunflo (Fig. 18A–D) is tentatively referred to *E.*? *thorslundi*. It is 27.9 mm long and although it has proportions close to those of typical but smaller examples on the "Big Block", the glabella is more elongate; it appears to have grown forward to the anterior border. If this identification is correct, it could be understood as part of a specimen of about the same size as the large trunk in Fig. 18E.

Generic assignment. – *Eccaparadoxides*? *thorslundi* is referred to the genus because the cranidium and pygidium show a general resemblance to those of typical *Eccaparadoxides*, but only with reserve because of differences in the glabella and the thorax. *E.*? *thorslundi* resembles typical *Eccaparadoxides* in the form of the glabella, which reaches but does not indent the anterior border in early holaspids, and in
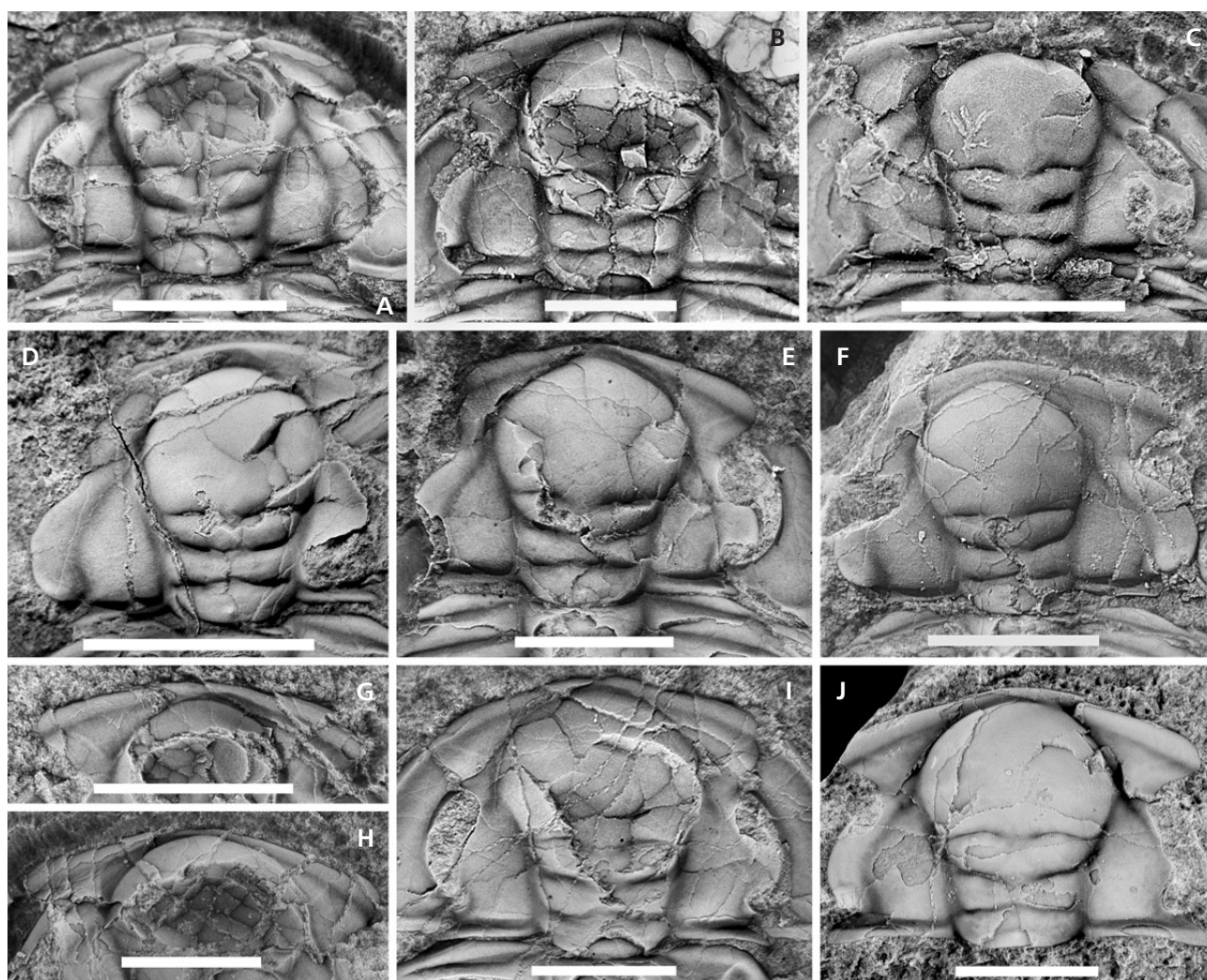
Figure 21. A–J – *Hydrocephalus spinulosus* sp. nov., cranidia. • A – PMU 25711/12, holotype. • B – PMU 25711/3, glabellar front rounded. • C – PMU 25711/91, S1, S2 well developed but S3 and S4 not developed. • D – PMU 25711/53, latex cast; shows occipital node and broad palpebral lobe. • E – PMU 25711/67, latex cast; glabellar front somewhat pointed. • F – PMU 25711/46, with narrow preglabellar field. • G – PMU 25711/41, and H – PMU 25711/35, show the preglabellar furrow confluent with the anterior border furrow. • I – PMU 25711/61, latex cast. • J – PMU 25671 from Östnår. Scale bars = 5 mm.

the long, curved palpebral lobes; but it differs from the type and several other species by not showing any appreciable trace of glabellar furrows S3 and S4 in the holaspid stages. The sub-hexagonal shape of the pygidium of *E.? thorslundi* recalls some species of *Eccaparadoxides*, but differs from several species because it is wider than long. In *E. pusillus* the pygidial length and width are about equal (Šnajdr 1958, pl. 22, figs 9–15), and in several other species it is markedly elongated (Courtessole 1973, pl. 9, figs 4, 6, 7; Esteve 2014, fig. 13). The pygidial shape, the length of the pygidial axis and the presence of a post-axial swelling in *E.? thorslundi* are comparable with those of *E. eteminicus* (Matthew), as figured by Kim *et al.* (2002, fig. 8:12–14).

The thorax of *E.? thorslundi* differs from those of typical *Eccaparadoxides* because the anterior pleurae are straight and nearly transverse with extensive pleural grooves and short backwardly-curved pointed pleural tips. In contrast, in *E. pusillus* (Šnajdr 1958, pl. 22, fig. 3), *E. insularis* (Westergård 1936, pl. 7, fig. 9) and *E. eteminicus* (Kim *et al.* 2002, fig. 7), the anterior pleurae curve backwards in a wide arc, almost from the axial furrow to the pleural tip; distal of the fulcrum, the pleural furrows fade out and the pleurae form nearly flat blades with a broad doublure (Fig. 10B), as in the above-mentioned species, and also in *E. pradoanus* (Verneuil & Barrande), well figured by Esteve (2014, fig. 5).

For the present we rely on cephalic and pygidial characters to place the species *thorslundi* provisionally with *Eccaparadoxides*?, rather than use thoracic characters to exclude it from that genus.
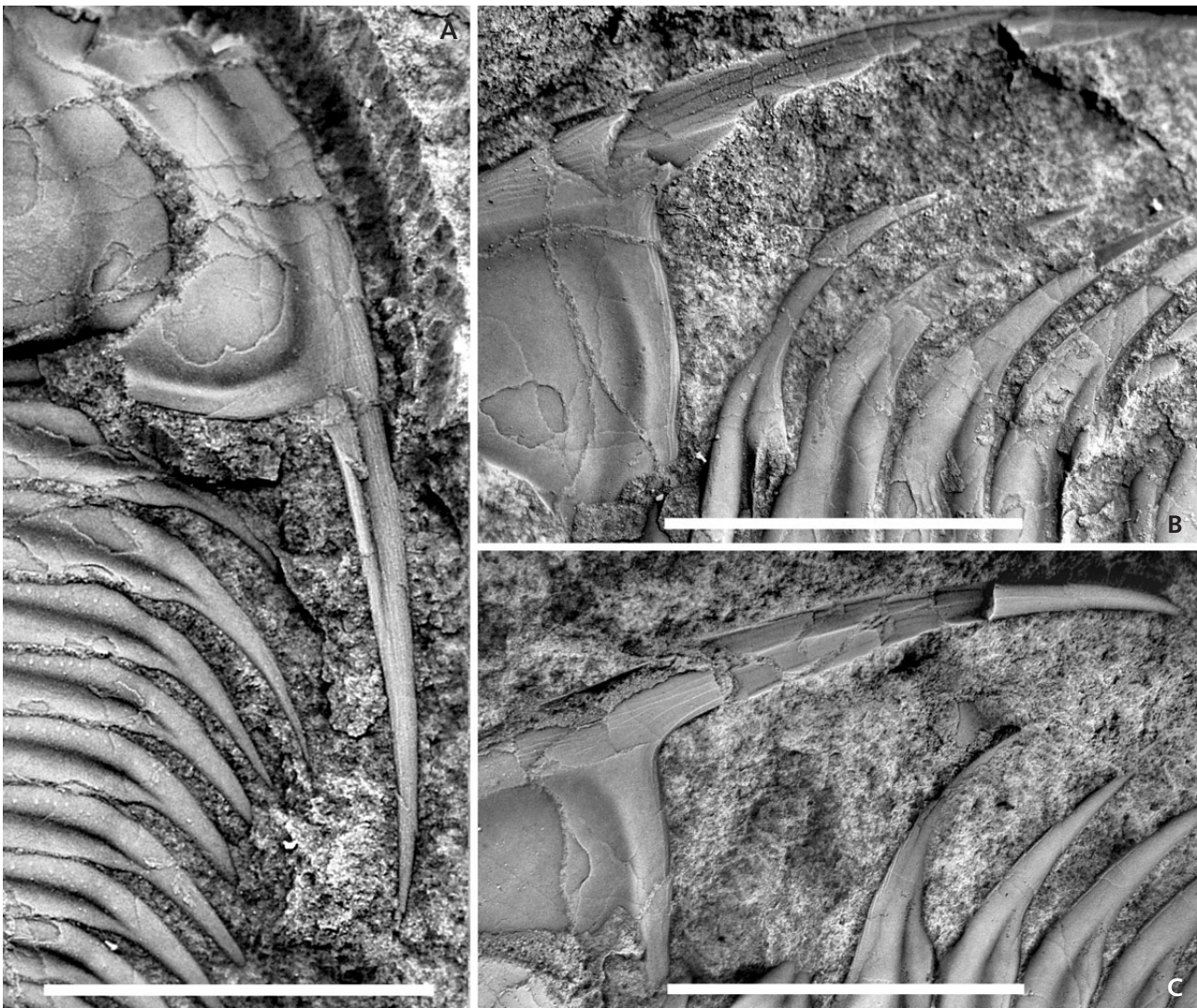
Figure 22. *Hydrocephalus spinulosus* sp. nov., librigenae. • A – PMU 25711/12, holotype. • B – PMU 25711/9, shows fine terrace-lines on the dorsal surface of the lateral and posterior borders and a mould of coarser ventral terrace-lines on the genal spine. • C – PMU 25711/61, latex cast. Scale bars = 5 mm.
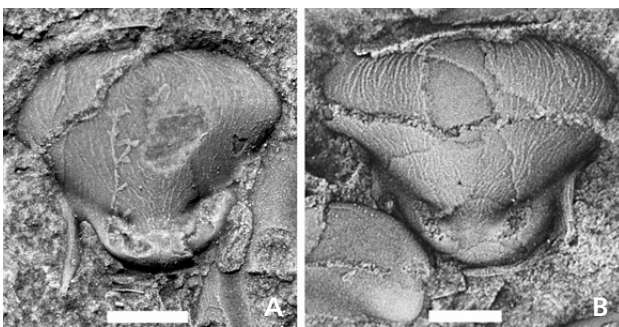

Figure 23. *Hydrocephalus spinulosus* sp. nov., hypostomata. • A – PMU 25711/53. • B – PMU 25711/46. Scale bars = 5 mm.

Comparison with other species. – As mentioned above, *E.? thorslundi*, in lacking clear glabellar furrows S3 and S4, differs from typical *Eccaparadoxides* species, inclu-

ding also *E. acadicus* (Matthew) and *E. lamellatus* (Hartt), as revised by Kim *et al.* (2002), and several species from Spain (Liñan & Gozalo 1986) and the Montagne Noire in France (Courtessole 1973).

In *E.? thorslundi* the palpebral lobe extends forwards and inwards to reach near to the glabella at its widest point (Fig. 11E); in doing so it passes between the glabella and point γ on the facial suture. This contrasts with some *Eccaparadoxides* in which the anterior end of the palpebral lobe terminates abruptly (Fig. 11I), and point γ lies just in front of it and very close to the glabella (Šnajdr 1958, pl. 20, fig. 46; pl. 21, fig. 5). In *E. pradoanus* (Verneuil & Barrande), as figured by Esteve (2014, figs 3, 4, 10), the facial suture is shown extending a short way exsagittally along the side of the glabella. This is an unusual course for a paradoxidid suture.

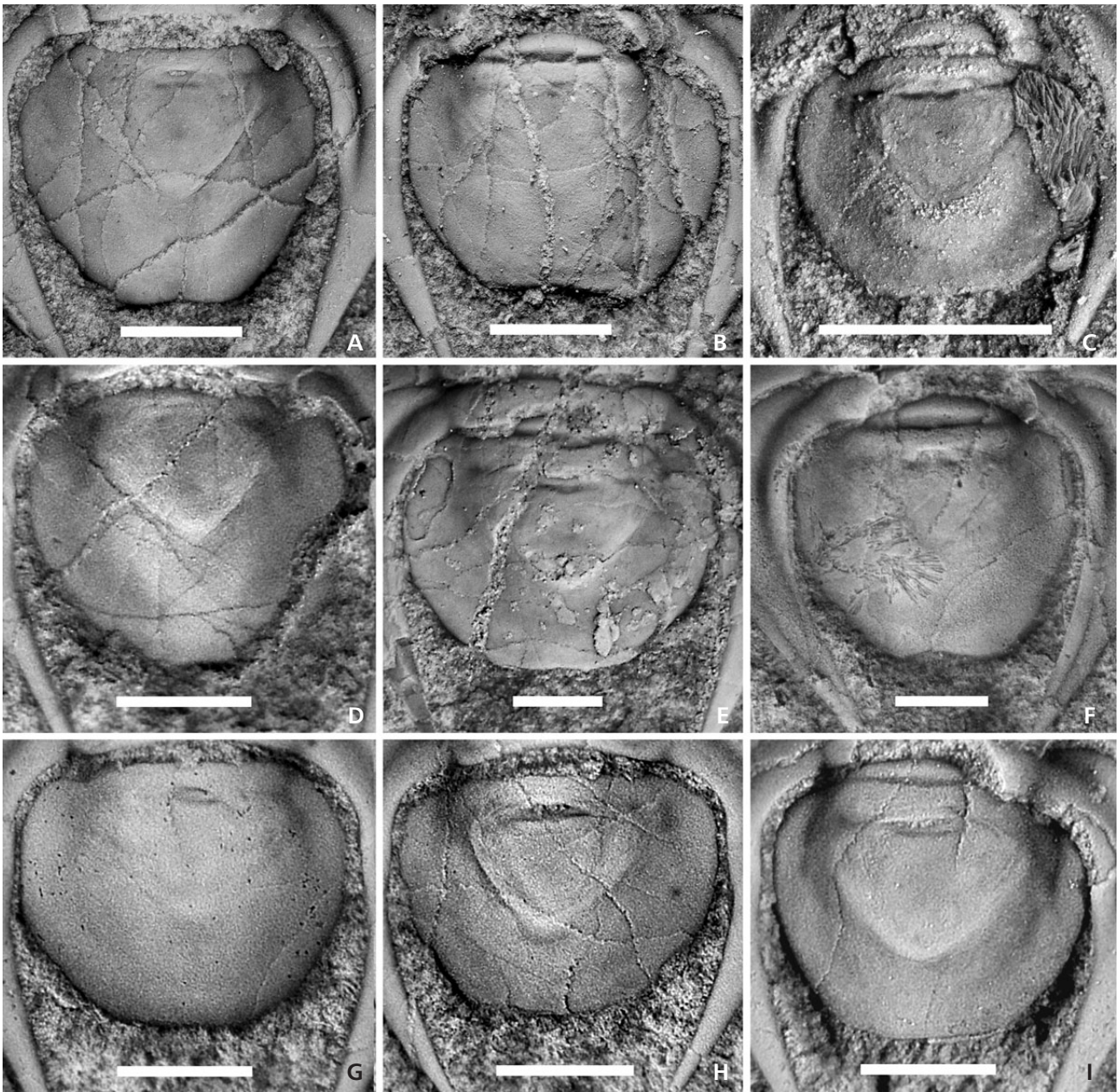There are several species of *Paradoxides* described

Figure 24. *Hydrocephalus spinulosus* sp. nov., pygidia, illustrating variation in outline and the degree of effacement of the axial furrows. • A – PMU 25711/22. • B – PMU 25711/2. • C – PMU 25711/91. • D – PMU 25711/57, latex cast. • E – PMU 25711/9. • F – PMU 25711/80, latex cast. • G – PMU 25711/61, latex cast. • H – PMU 25711/62, latex cast. • I – PMU 25670, from Östnår. Scale bars = 1 mm.

from Poland and Siberia whose cranidia show clearly only glabellar furrows S1 and S2; most of those have narrower interocular genae than *E.? thorslundi*. Orłowski (1965, 1985) illustrated cranidia of several such species, among which *P. slowiecensis* has a short anterior border exsagittally, much like *E.? thorslundi*, and weakly incised S3 and S4; but it differs because the interocular genae are considerably less wide (tr.) and the palpebral lobes are less long. Among the Siberian species, *Paradoxides ruminatus* Fedjanina (*in* Chernysheva 1971, p. 97, pl. 3, fig. 6), from

the lower Amgan strata of the river Amzass, has similar proportions to *E.? thorslundi*, but the glabella has straight (not concave) lateral margins, the palpebral lobes are more regularly curved, and the preocular genae are less expanded. The cranidium of "*Paradoxides* sp. 2" in Savitsky *et al.* (1972, pl. 11, fig. 7), from the *Oryctocara* Zone at the base of the Amgan Stage as exposed in the Nekekit River, Siberia, resembles *E.? thorslundi* in glabellar shape and the proportions of the fixigenae, but differs in having a much wider anterior border (sag.,

exsag.). The fixigenae, palpebral lobes and narrow frontal border of *Paradoxides hyperboreus* Lermontova (Jegorova *et al.* 1982, pl. 54, fig. 11) resemble those of *E.? thorslundi* but the anterior part of the glabella is much more extended, being ogival in outline and relatively sharply rounded in front.

Genus *Hydrocephalus* Barrande, 1846

Type species. – *Hydrocephalus carens* Barrande, 1846, subsequently designated by Šnajdr (1958, p. 129).

Remarks. – The lectotype of *H. carens* (Šnajdr, 1958, pl. 24, fig. 32) is a meraspid of "degree" 8 or 9 whose sagittal length is a little over 3.3 mm, the cephalon having a length of about 1.8 mm. It is from the Buchava Formation at the locality Pod hruškou, Týřovice, Czech Republic. Barrande (1852) and subsequent workers have collected a large number of additional specimens from the same formation, and these have enabled a reconstruction of the ontogeny (*e.g.* Šuf 1926; Šnajdr 1958, pl. 22, text-figs 24, 25). Fully grown specimens of *H. carens* attain a great size: the largest trunk illustrated by Barrande (1852, pl. 11) is 180 mm long and, if the cephalon of corresponding size were added, the length of the whole exoskeleton would approach 300 mm.

One of the most remarkable features of *Hydrocephalus carens* is the nearly circular outline of the meraspid glabella. However, this special feature has not so far been found in any other species of *Hydrocephalus*, though it is suggested by the glabella of small specimens of *H. minor* (Boeck) figured by Šnajdr 1958 (pl. 23, figs 1, 2). The sister-group of *Hydrocephalus* is not known at present, but the account by Dean & Rushton (1997, p. 476) gave a fairly accurate idea of the genus as used at the time that they were writing, and this is adopted here.

Hydrocephalus spinulosus sp. nov.
Figures 20A, 21–28, 29A, C, F, 30A, 31A

> 2007 *Hydrocephalus vikensis* sp. nov. (part); Rushton & Weidner, pl. 3, figs 6, 7?.
> 2013 Paradoxidid sp. 1; Ebbestad *et al.*, p. 20, figs 3B, C, 6B, D, 8A, B.

Holotype. – PMU 25711/12 (Fig. 20A), a dorsal shield about 21 mm long.

Material. – 28 fairly complete articulated exoskeletons on the "Big Block" (PMU 25711) from Tännberget quarry, Östnår, Jämtland (Ebbestad *et al.* 2013); also several other fragmentary specimens from Östnår, Travbanan (Hackås), Mon, Klocksåsen and Brunflo. A doubtful specimen was collected at Våle. The specimens from the principal surface of the "Big Block" are small holaspids of sagittal length 17 mm to 35 mm.

Etymology. – From the long and slender pleural spines.

Diagnosis. – *Hydrocephalus* with relatively long and broad palpebral lobes; width of cranidium across preocular genae (β–β) generally less than the width across palpebral lobes (δ–δ); thorax with maximum width a little more than its sagittal length, and generally comprising 18 segments; the pleural spines are long and curve backwards, the anterior segments in particular having long, thin and widely arcuate pleural spines; they do not show articulating processes; pygidium rather variable, small, semi-oval, with width/length about 1.2:1; axis commonly rather diffuse, some show one axial ring, others are not clearly segmented. The species is known only from specimens of small size < 36 mm long.

Description. – Exoskeleton oval in outline, the cranidial length about one third of the sagittal length and the greatest width across the thorax about 2/3 of the overall sagittal length. The length of the pygidium is about 7% of the length of the exoskeleton.

Cranidium wider than long (ratio about 1:0.7). Glabellar length nearly 4/3 of its maximum width. Glabella widens forward only slightly from LO to S2, then more strongly forward of S2 to reach a maximum width about 1.5 times that of LO (average 1.48, range 1.35 to 1.62, $n = 28$; Fig. 8B). Glabellar front generally bluntly rounded (Fig. 21B), but in some specimens a little more sharply rounded at the mid-line (Fig. 21E); lateral outline of glabella in dorsal view is gently concave. Occipital ring (LO) longest medially, shorter (exsag.) towards the axial furrow; a weak occipital tubercle is commonly visible towards the posterior edge of LO (Fig. 21A, D). SO deep laterally, shallower medially where it is bowed forwards. S1 deep laterally where it is directed inwards and obliquely slightly backwards, the median part is often markedly shallower where it crosses the glabella (Fig. 21C, F); the connection with the axial furrow may be weak. S2 deep laterally, but more finely incised than S1; it may be weakly connected across the glabella, but is commonly disjunct. Each half of S2 is nearly transverse, but may be slightly

Figure 25. *Hydrocephalus spinulosus* sp. nov. • A – PMU 25711/61, latex cast. The pathological condition of part of the thorax was discussed by Ebbestad *et al.* (2012, p. 22). • B – PMU 25711/79, latex cast. • C – PMU 25711/67, latex cast. • D – PMU 25711/57, latex cast. Scale bars = 5 mm.
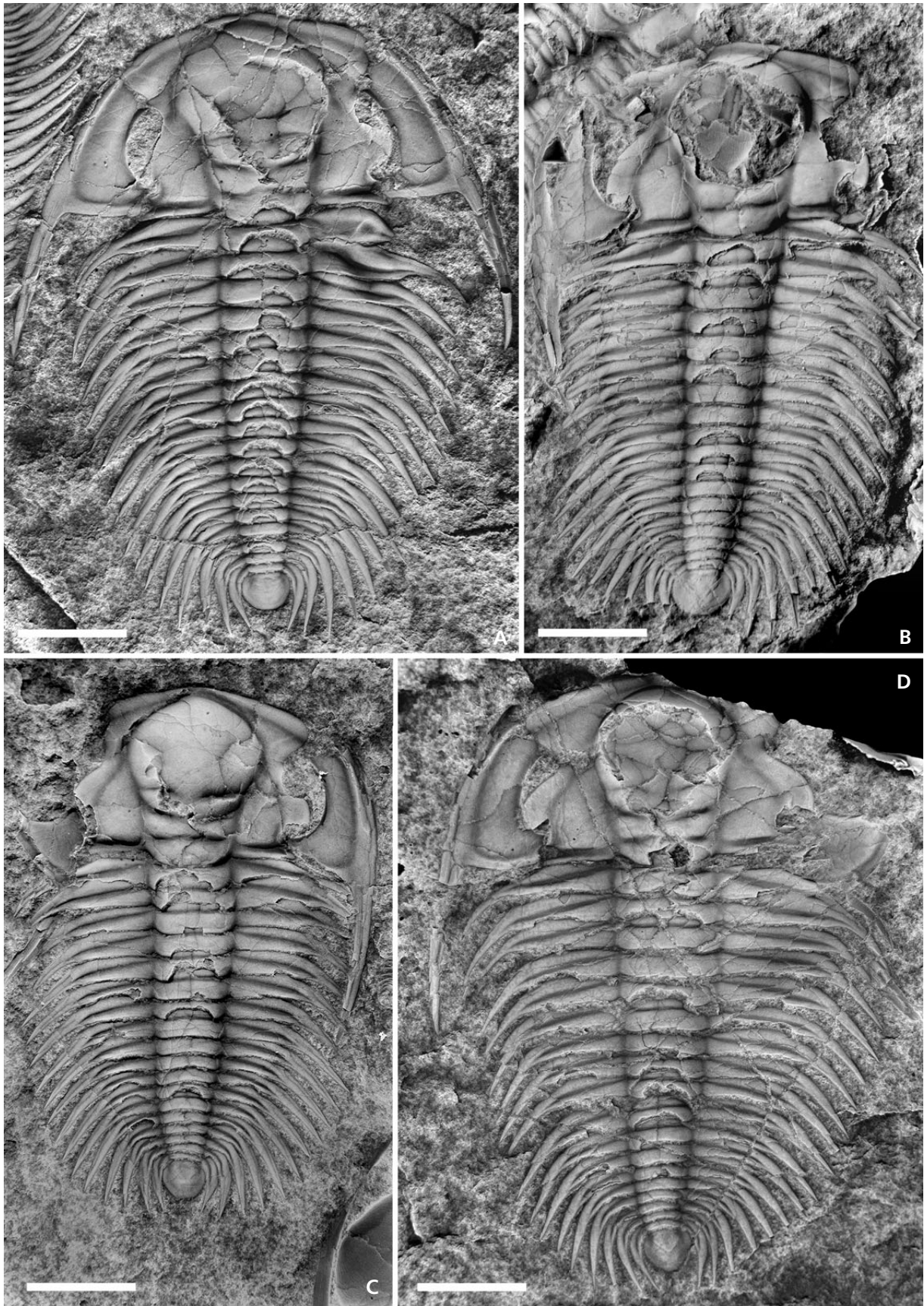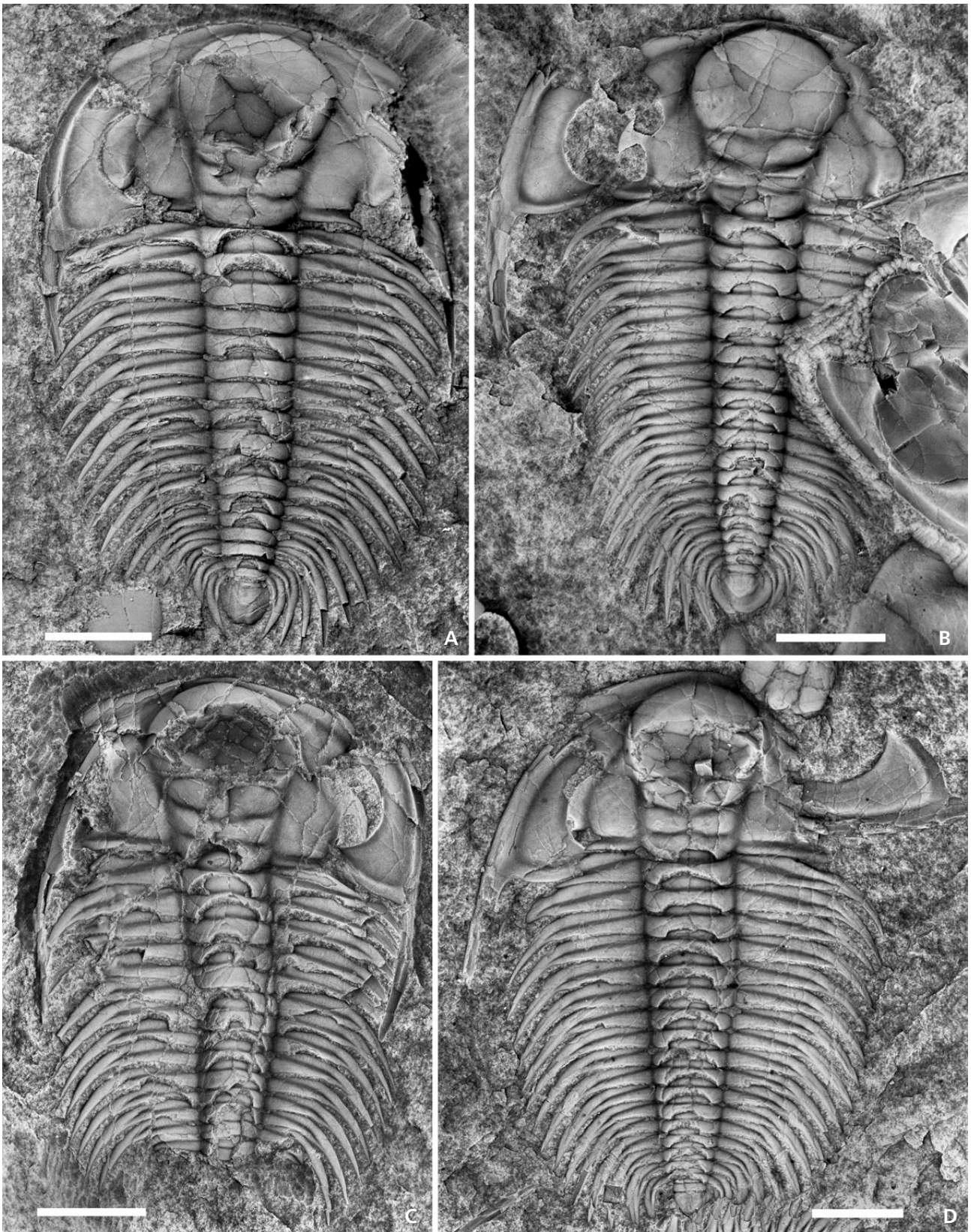
Figure 26. *Hydrocephalus spinulosus* sp. nov. • A – PMU 25711/22. • B – PMU 25711/75, latex cast. • C – PMU 25711/35. • D – PMU 25711/3. Scale bars = 5 mm.
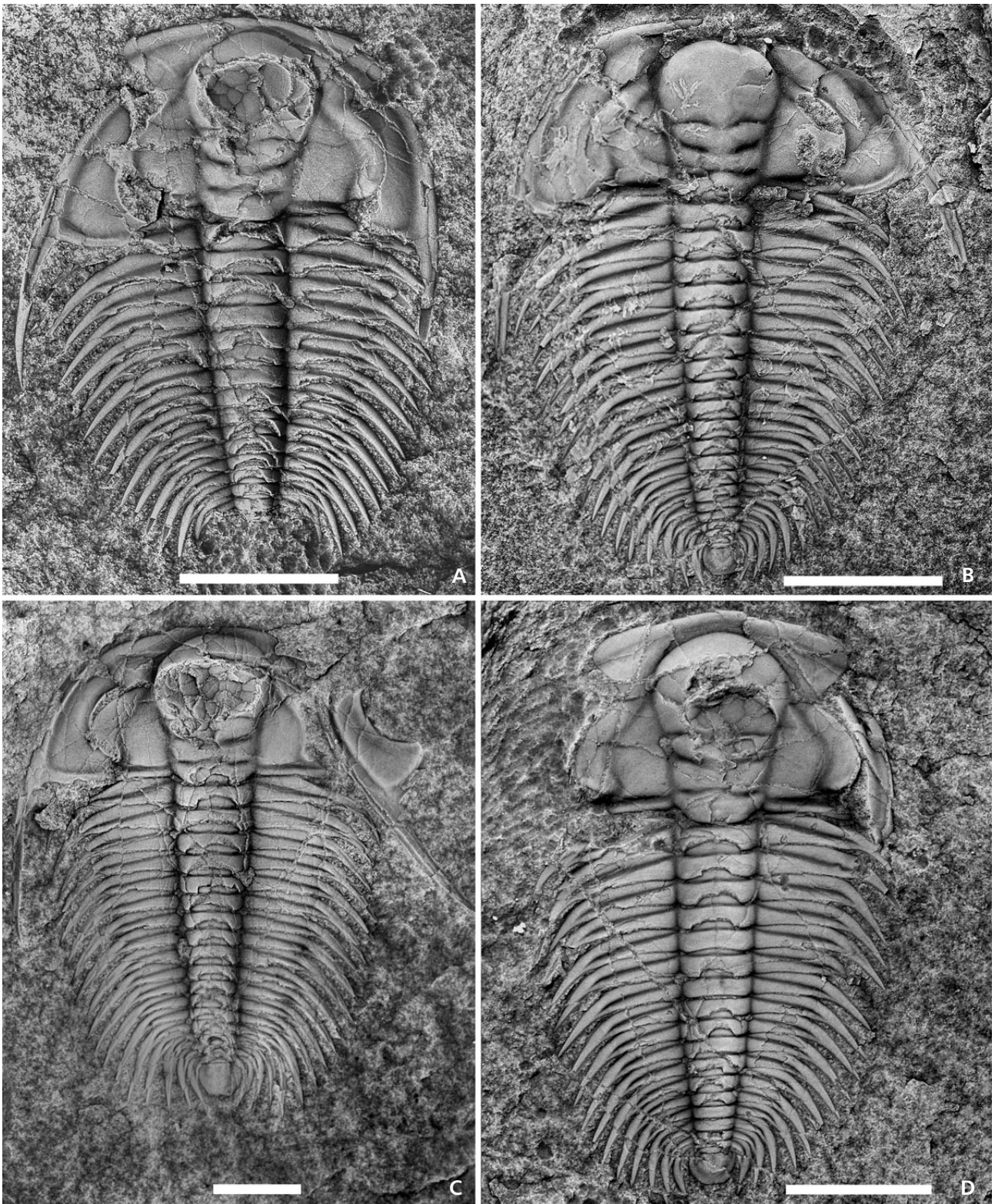
Figure 27. A–D – *Hydrocephalus spinulosus* sp. nov. • A – PMU 25711/41. • B – PMU 25711/91. • C – PMU 25711/2, a moult configuration in which the right librigena became inverted laterally. • D – PMU 25711/37. A small holaspid with 17 thoracic segments referred to the species (see also text for comparison with *H. vikensis*). The cranidium 7.5 mm long, showing narrow preglabellar field. Scale bars = 5 mm.

bowed forwards. S3 and S4 not evident (Fig. 21C, F). Some specimens show faint raised lines on the frontal glabellar lobe, approximately concentric with the course of the furrow round the front of the glabella (Fig. 28E).

Frontal area short sagittally, averaging 7.5% of glabellar length in holaspids more than 20 mm long, in which the glabella reaches the border furrow (Fig. 21A, J) and may impinge on the anterior border medially (Fig. 21E, H). A short preglabellar field may be present in small cranidia (Fig. 21F, 7 mm long). Anterior border furrow shallow and may be indistinct (Fig. 26A). Border slightly convex in longitudinal profile, widening slightly away from the mid-line. The width of the preocular genae (β–β) is slightly less wide than the width across the palpebral lobes (δ–δ) (Fig 8C). Preocular facial line seen only in small cranidia (Fig. 28B). Point γ at the anterior end of the ocular section of the facial suture usually lies just a little posterior to the widest part of the glabella and is set distally from the axial furrow by about a quarter of the maximum glabellar width (Figs 21A, 26A). The palpebral lobe originates close to the widest part of the glabella and extends posterolaterally in an uneven outwardly convex curve, becoming broader posteriorly, near to point γ, behind which it curves inward a little and ends above and slightly in advance of the posterolateral border furrow (Fig. 21J). The length of the palpebral lobe in the larger specimens is less than half the glabellar length (about 45%), but in a small specimen, < 20 mm long, is proportionately a little longer (> 50%). The maximum width of the interocular gena, from axial furrow to palpebral furrow, is about half the width of L1, or a little more. The maximum width of the palpebral lobe is about half that of the interocular gena, or in some specimens more than half (Fig. 21D, F). The postocular suture is short and oblique. The postocular gena has about the same transverse width as LO.

Librigena somewhat narrow; the smallest width between the ocular incisure and the outer margin is about equal to half the length of the ocular incisure, or commonly slightly less. The genal field is about twice as wide as the lateral border (Fig. 26B). The posterior border is narrower than the lateral border, gently curved convexly backwards; both the lateral and posterior borders bear dorsally a few very fine terrace-lines parallel to the margin (Fig. 22B, C). The inner spine angle is slightly obtuse. The genal spine curves slightly inwards posteriorly (Figs 22A, 25D) and has about four relatively coarse terrace lines on its ventral surface (Fig. 22B).

Hypostomes differing from that assigned to *Eccaparadoxides*? *thorslundi* in their less transverse shape are tentatively assigned to the present species (Fig. 23). The middle body is, in outline, a little more than a quadrant and has a whorl of terrace-lines centred towards the anterior edge. The hypostome is rounded anteriorly and the posterior lobe of the middle body crescentic in outline. The maculae are small and the marginal spine seen is long and thin.

Thorax of 18 segments with relatively long and slender pleural spines. The anterior segment has a deep and wide pleural groove and a fulcrum relatively close to the axial furrow (Figs 20A, 25D, 27B); distally the pleura narrows to form a slender spine that extends abaxially considerably further than the width of the axial ring and makes a wide curve outwards and backwards (Figs 20A, 26D), commonly as far back as the third axial ring or the junction of the third and fourth rings; the second segment usually has similarly arcuate pleurae. Subsequent pleurae are curved more posteriorly and the spines extend less far laterally than the anterior ones (Fig. 26D). The pleurae have an ill-defined fulcrum that is distant from the axial furrow by rather less than the width of the corresponding axial ring; no articulating process is seen, and the manner in which the segments articulated has not been discerned in detail. Distally the pleurae all have long, tapering pleural spines that are directed progressively more strongly backwards in the more posterior segments, and, as preserved, the pleural spines are characteristically splayed out with distinct interspaces between them (Fig. 25D). The pleural grooves extend into the bases of the spines. The spines of the last four segments extend further back than the posterior edge of the pygidium (Fig. 25A–D). Some well-preserved segments show a finely granulate surface on the pleurae, including in the pleural groove and on parts of the axial ring. There are larger and more widely spaced granules (but still very subdued) forming an irregular line on the propleurae (Fig. 28F); these may be usual for the species but are not seen in many examples. The doublure of the thoracic segments has not been seen. One specimen (Fig. 25A) shows striking malformations of the thorax, as was discussed by Ebbestad *et al.* (2013, p. 22, fig. 8).

Pygidium variable (Fig. 24), a little wider than long (the average for 17 specimens is 1.22:1), rounded in outline or semi-oval, narrowing posteriorly; the posterior margin may be truncate or emarginate (Fig. 24A, B). Axis short, often indistinct, about 2/3 of the width of the pygidium and nearly 2/3 of its length. One axial ring is seen, clearly or only indistinctly. Some pygidia show a

Figure 28. *Hydrocephalus spinulosus* sp. nov. • A–D – juvenile specimens. • A – PMU 25711/50. • B – PMU 25711/89, latex cast. • C – PMU 25711/68, latex cast of a late meraspid. • D – PMU 25711/46, a small holaspid. • E – PMU 25671, a cranidium from Östnår. Detail of ornamentation on glabella. • F – PMU 25711/12, holotype, detail of ornamentation on 3rd and 4th right pleural fields. Scale bars = 1 mm.
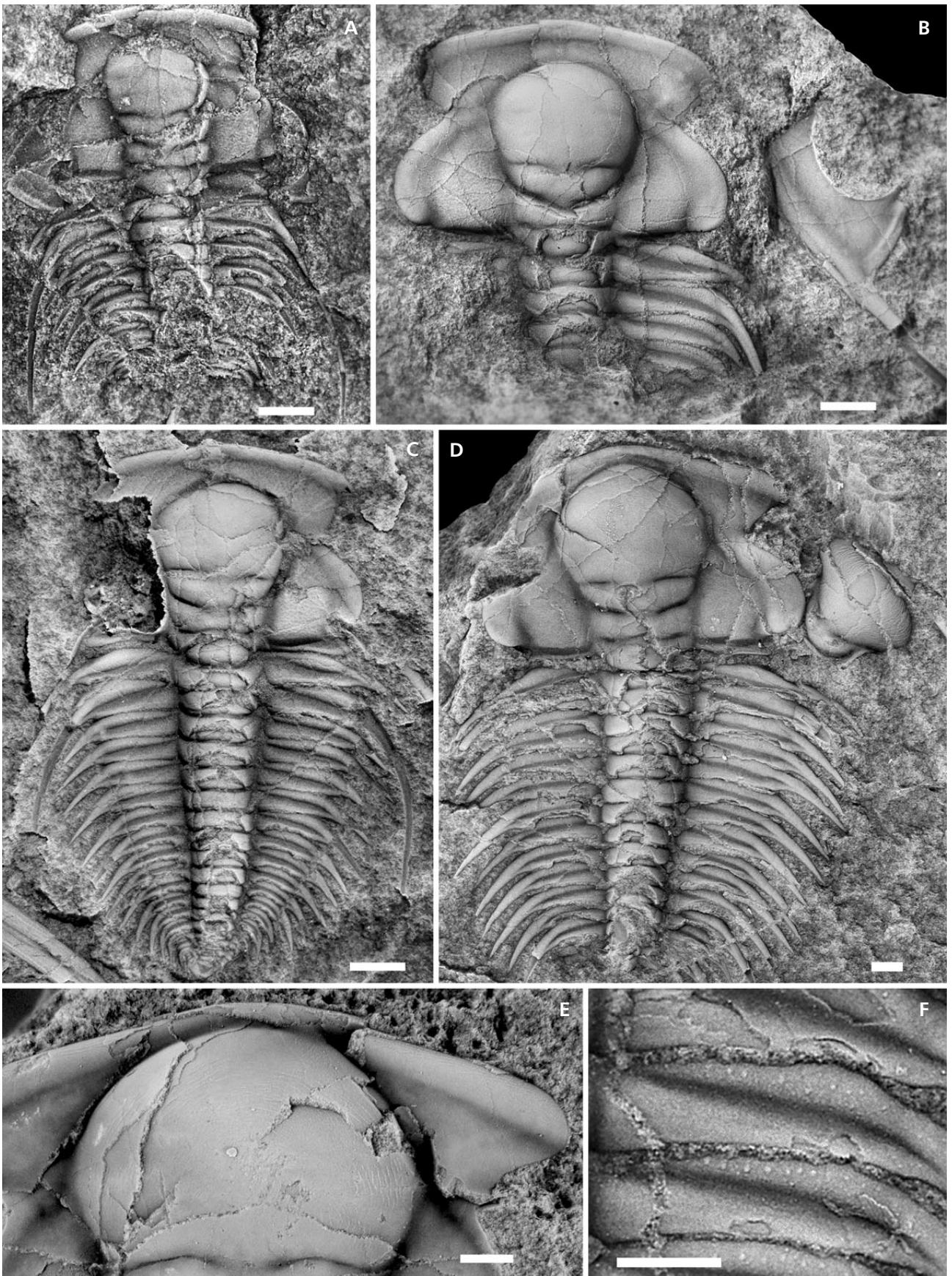
Table 8. Juvenile specimens on the principal surface of the Big Block that are referred to *Hydrocephalus spinulosus*.

Fig.	Cranidial length (mm)	Remarks
28A	3.5	Frontal area about 17% of cranidial length, 1st segment fragmentary, long spine on 2nd segment. Occipital node distinct.
28C	3.8	Frontal area 18% of cranidial length, 16 spinous segments seen, the 2nd with a long spine, + transitory(?) pygidium.
28B	4.3	Frontal area 18% of glabellar length. Irregular row of granules on the propleura of segments 3 and 4.

post-axial swelling (Fig. 24D), others do not (Fig. 24E). No clear border or pleural furrows are seen. The doublure was not observed.

Juvenile specimens. – A few specimens appear to be referable to *Hydrocephalus* (as used here) and are presumed to represent the common species on the "Big Block", namely *H. spinulosus* (see Table 8).

Measurements. – The holotype (25711/12; Fig. 20A) has a sagittal length of 20.9 mm and a cranidial length of 7.2 mm. The largest exoskeleton on the "Big Block", PMU 25711/80 (not figured), is 35.3 mm long, the cranidium being 11.7 mm and the pygidium 2.6 mm long. We have not yet recognised significantly larger sclerites of *H. spinulosus* from the other localities in Jämtland where the species has been collected.

Generic assignment. – *Hydrocephalus spinulosus* much resembles *H. vikensis* Rushton & Weidner (2007). Those authors had compared *H. vikensis* with *Hydrocephalus minor* (Boeck), a species that is fairly typical of *Hydrocephalus* Barrande. Both *H. carens* and *H. minor* have palpebral lobes of regular curvature and fairly even breadth (Šnajdr 1958, pl. 23, pl. 25, fig. 21; Rushton & Weidner 2007, pl. 2, figs 2, 9). The plentiful material of *H. spinulosus* and some new specimens of *H. vikensis* show that the palpebral lobes of those two species differ from *H. carens* and *H. minor* because their palpebral lobes are less regularly curved, extending backwards and outwards from near the widest part of the glabella, becoming broader as they reach point δ on the ocular suture, whence they become more strongly curved adaxially at their posterior ends. Palpebral lobes of this sort are a feature of a group of Siberian *Paradoxides* species

known mainly from cranidia only, that were recognised by Geyer & Vincent (2014, p. 24) as forming an unnamed clade of paradoxidids. With the specimens available it is not possible to assess fully the relationships of *H. vikensis* and *H. spinulosus* with the Siberian clade, nor with the Bohemian crown-group *Hydrocephalus*; but if early meraspids of the latter two Jämtland species were found, they might provide decisive evidence.

Comparison with Hydrocephalus vikensis. – *Hydrocephalus spinulosus* is generally similar to *H. vikensis* and most of the distinctions we have observed in the cephalon and pygidium are quite small (Fig. 29). The main distinctions lie in the thorax: the simplest observed difference is that holaspids of *H. vikensis* have 17 thoracic segments and holaspids of *H. spinulosus* have 18; to apply this obviously demands suitably preserved dorsal or axial shields. Rushton & Weidner (2007, p. 397) recorded six 17-segment specimens in the type material of *H. vikensis*, and two additional examples have since been identified. On the "Big Block", a number of the moulted *Hydrocephalus* exoskeletons are disarranged, with the pygidium missing or the posterior thoracic segments telescoped, so that the number of segments is uncertain; but there are about sixteen specimens of *spinulosus* in which 18 segments can be counted, while there are no definite examples with more than 18, and only one with 17 segments (see Fig. 27D). However, this distinction remains inconclusive because the number of thoracic segments is known to vary within some paradoxidid species (Bergström & Levi-Setti 1978, Esteve 2014), whereas it appears to be constant in others (*fide* Westergård 1936, p. 33; Westergård 1953, p. 35). One small holaspid (Fig. 27D) is anomalous: the thorax is typical of *H. spinulosus*, but with only 17 segments; the anterior segment is only partly preserved, but it resembles the first segment of most *H. spinulosus*, in that the right-hand pleura has a relatively deep and wide pleural furrow, and appears to have a fulcrum like those seen in the holotype and other specimens. This specimen is referred to *H. spinulosus*.

In *H. vikensis* the anterior thoracic pleurae are more or less transverse. With favourable preservation, or removal of part of the preceding pleura, an articulating process is seen at the anterior edge of the pleura (Fig. 31B), as also in *H. carens* (Whittington 1990, p. 40, fig. 21), and from this point the pleurae bend rather abruptly obliquely backwards and outwards to form pleural spines; the spines are nearly

Figure 29. A, C, F – *Hydrocephalus spinulosus* sp. nov. • A – PMU 25711/75, latex cast. The white arrow shows the point γ on the facial suture. • C – PMU 25711/12, the anterior pleural spines of the holotype. • F – PMU 25711/39. • B, D, E, G – *Hydrocephalus vikensis* Rushton & Weidner, 2007. • B – PMU 26076, dorsal view of a cranidium from Viken, loc. 2 (Rushton & Weidner 2007, p. 392, fig. 1d); see also Fig. 30C, D. • D – PMU 25711/11, thoracic segments 4 to 7 (see Fig. 20B). • E, G – NRM-PZ Ar60130a. • E – thoracic segments 3 to 7, and G – pygidium of the holotype, original of Rushton & Weidner (2007, pl. 1, fig. 11). Scale bars in A–E = 5 mm; in F–G = 1 mm.
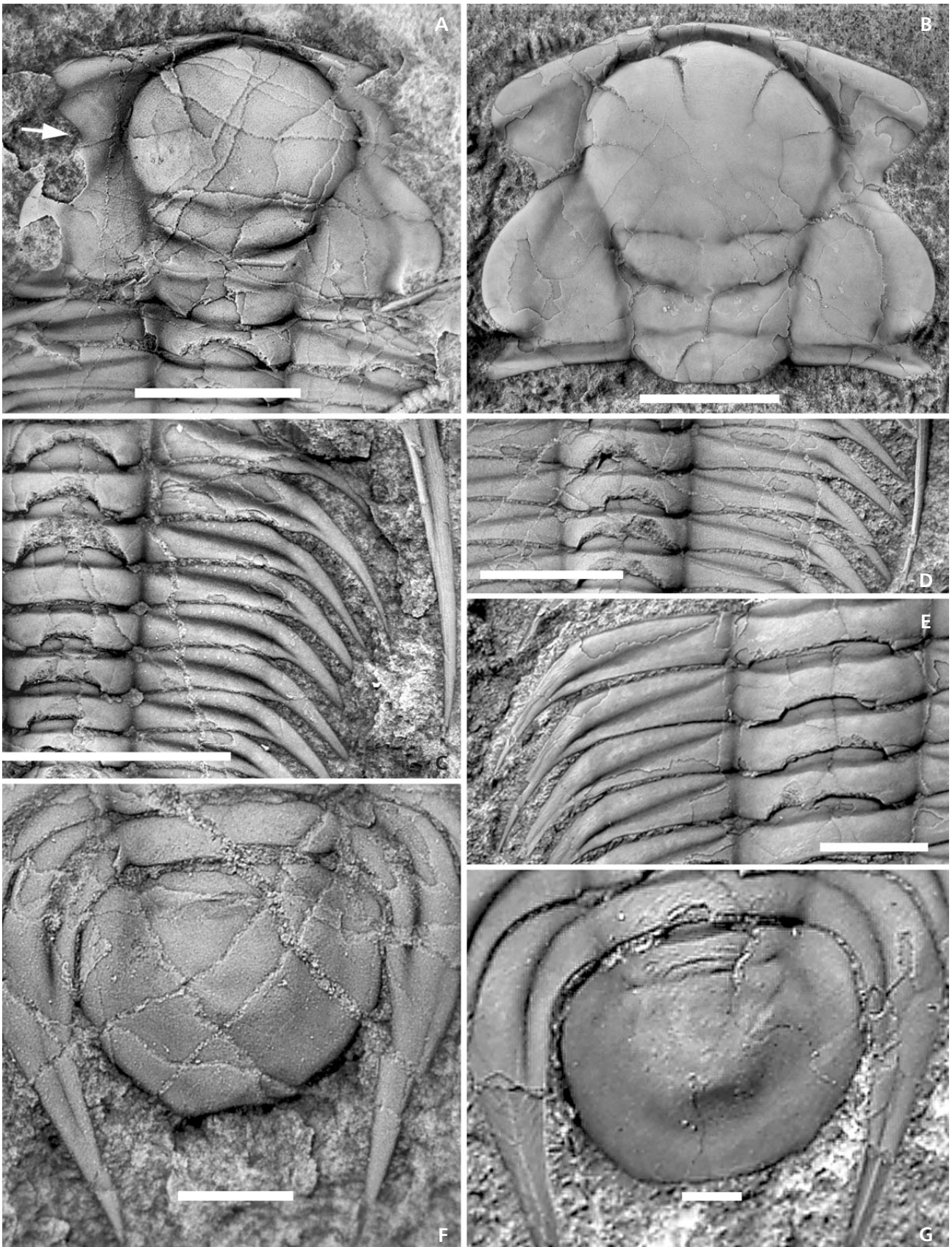
straight and tend to lie close together, with slight interspaces, as seen in other species of *Hydrocephalus*. In *H. spinulosus* the thoracic pleurae bend smoothly backwards to form long curved spines that may be somewhat separated or splayed out (Fig. 25D). The anterior two segments have long and strikingly curved pleural tips (Figs 20A, 22, 26). No articulating process has been observed in *H. spinulosus* and it is not known in detail how the thoracic segments articulated. The posterior parts of the thorax in the two species are more similar.

The thorax of *H. vikensis* is about the same length sagittally as its maximum width (average length/width = 1.03, range 0.97 to 1.05, $n = 5$); even though the thorax of *spinulosus* has one extra segment, it is proportionally shorter, being wider than its sagittal length (average length/width = 0.87, range 0.83 to 0.91, $n = 15$).

As mentioned in the section on statistical analysis (above), linear measurements made on the cranidia of the two taxa showed no significant differences (Fig. 8). In *vikensis*, point γ on the facial suture generally lies less far forward than the widest part of the glabella, whereas in *spinulosus* the point γ tends to lie almost as far forward as the widest part of the glabella (Fig. 29A, B); this distinction is less clear in small specimens.

The pygidium of *H. vikensis* has an average width 1.35 times the length (excluding the articulating half-ring), based on 12 specimens, and has a distinct axis with one clear axial ring; usually one short pleural groove is visible (Fig. 29G; Rushton & Weidner 2007, pl. 3, figs 15, 16); there is no border, but there is a narrow down-sloping rim or fascia around the posterior part of the pygidium (Rushton & Weidner 2007, pl. 3, figs 14, 16, 19). The pygidium of *H. spinulosus* is a little narrower, the width averaging 1.22 times the length ($n = 17$) and the axis is commonly less distinct, sometimes merging into a post-axial swelling (Fig. 29F). Some pygidia of *H. spinulosus* have a slight embayment in the posterior margin that has not been seen in *H. vikensis*; however some other specimens of *spinulosus* have a pygidium quite similar to that of *vikensis* (Fig. 24E).

Comparison with other species. – *Hydrocephalus sjoegreni* (Linnarsson), as illustrated by Westergård (1936, pls 9, 10), shows glabellar furrows S3 and S4 at a range of sizes and has palpebral lobes of even breadth, as in *H. carens*. The pygidium differs from that of *H. spinulosus* in widening posteriorly. *Hydrocephalus* sp. A of Weidner *et al.* (2014, p. 525) is known only from large cranidia: those have proportionally shorter palpebral lobes than *H. spinulosus* (as might be expected in large cranidia) and they are less recurved posteriorly. The anterior border is wider (exsag.) and more sharply defined. "Pygidium 2" of Weidner *et al.* (2014, fig. 15K–T), which those authors surmised might be the pygidium of *H.* sp. A, widens posteriorly,

whereas in *H. spinulosus* the pygidium narrows posteriorly.

Paradoxides rozanovi Jegorova (*in* Jegorova *et al.* 1976, p. 72, pl. 24, figs 1–6), from the Amgan Stage of the River Lena, is a large species that has a glabella and palpebral lobes comparable to those of *H. spinulosus*, and the interocular genae are comparably wide. *P. rozanovi* differs in having wider preocular genae (β–β) and a longer (sag., exsag.) frontal border. Among the Siberian *Paradoxides* species from the Amgan Stage in the Sayan-Altai region, *P. priscus* Poletaeva (*in* Chernysheva 1971, p. 97, pl. 4, figs 1–5) has glabellar furrows and palpebral lobes comparable with those of *Hydrocephalus spinulosus*, but the frontal area is longer and the doublure suggests that the cephalic border is considerably wider. The cranidium of *Paradoxides convexus* Fedjanina (*in* Chernysheva 1971, p. 96, pl. 4, fig. 8) has glabellar features similar to *H. spinulosus*, but the frontal border is more marked and the interocular genae are narrower.

Hydrocephalus vikensis Rushton & Weidner, 2007
Figures 20B, 29B, D, E, G, 30B, C, D, 31B

?1936 *Paradoxides* sp. No. 4; Westergård, pl. 7, fig. 13.

2007 *Hydrocephalus vikensis* sp. nov.; Rushton & Weidner, p. 396, pl. 1, figs 11–15; pl. 2, figs 1, 3–8; pl. 3, figs 1?, 2?, 3–5, 8–19 (not pl. 3, figs 6, 7?, = *H. spinulosus*).

2007 *Hydrocephalus* n. sp. (Typ 1); Münder, p. 144, fig. 2.

2011 *Hydrocephalus vikensis* Rushton & Weidner, 2007. – Weidner & Ebbestad, p. 73, fig. 1.

2014 *Hydrocephalus vikensis* Rushton & Weidner, 2007. – Weidner *et al.*, p. 525, fig. 13A, B, C?, D?, E?.

Holotype. – NRM-PZ Ar60130, a slightly disarranged axial shield about 60 mm long (Rushton & Weidner 2007, pl. 1, figs 11, 14, pl. 2, fig. 4), from the lower part of the Alum Shale Formation, locality 2 at Viken, Näkten, Jämtland, Sweden.

New material. – Two specimens from the principal surface of the "Big Block" from Tännberget quarry, Östnår; several specimens, mostly fragmentary, from the same locality and from Myssjö, Travbanan (Hackås), Hambergstorpet, Mon and Klocksåsen, Jämtland. Outside Jämtland the species occurrs on Tåsjö mountain in Ångermanland (Fig. 2C; see Weidner *et al.* 2014); and a pygidium from Borgholm, Öland (Westergård 1936, pl. 7, fig. 13) is possibly referable to *H. vikensis*.

Revised diagnosis. – A species of *Hydrocephalus* with relatively long and broad palpebral lobes and short postocular sutures; width of cranidium across preocular genae
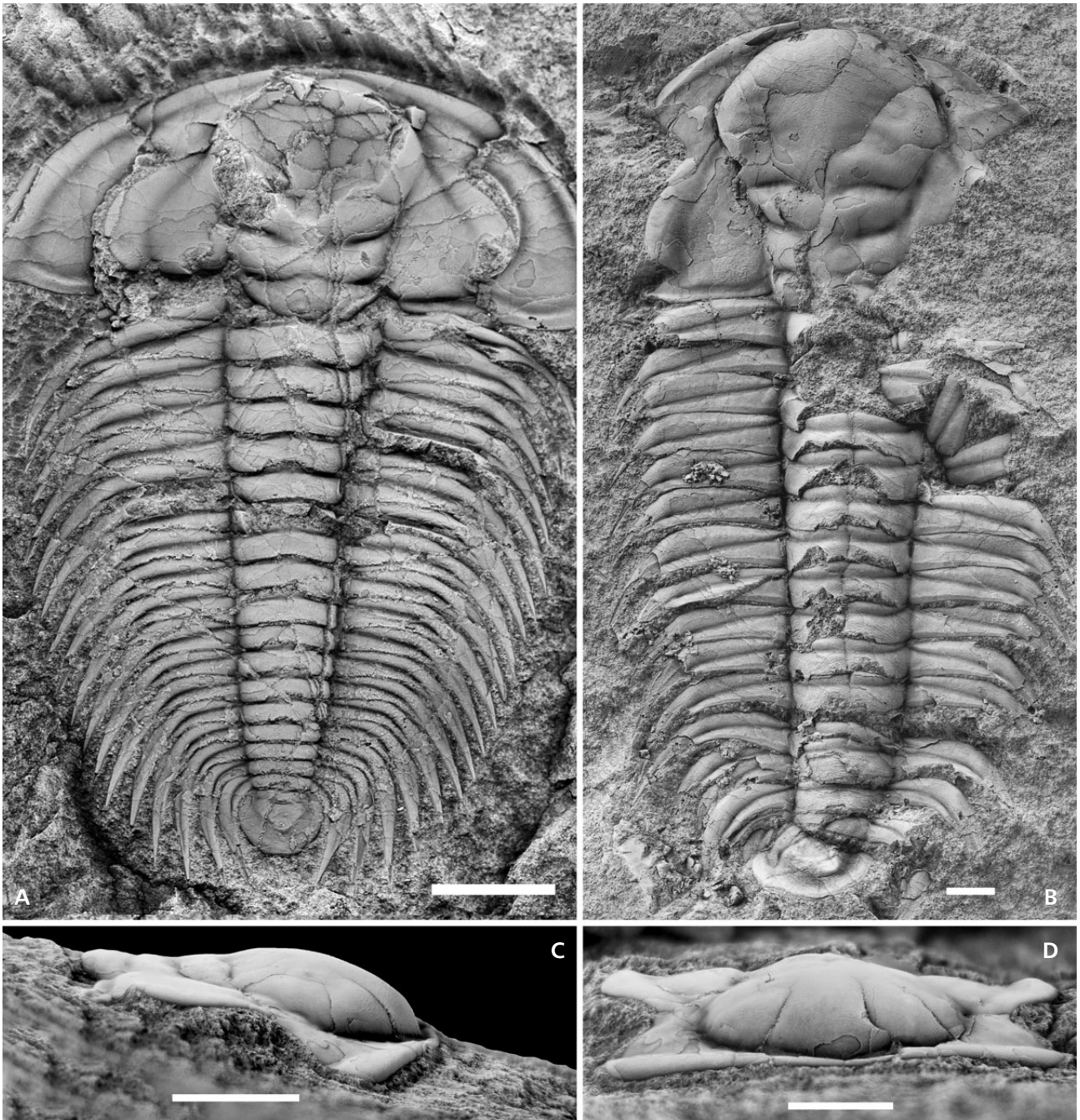
Figure 30. Comparison of the thorax. • A – *Hydrocephalus spinulosus* sp. nov. PMU 25711/9, one of the longest specimens. • B – *Hydrocephalus vikensis* Rushton & Weidner, 2007. NHMUK It 29216 (collected by T. Weidner) from Mon, south of Viken [photo by P. Crabb, © NHM]. • C, D – right lateral and frontal views of the cranidium shown in Fig. 29B, PMU 26076. All scale bars = 5 mm.

(β–β) nearly the same as width across the palpebral lobes (δ–δ); thorax with maximum width nearly equal to its sagittal length, composed of 17 segments with long and sharp pleural spines; the anterior spines bend abruptly back from the transverse line and are nearly straight; pygidium wider than long (about 1.35:1) with one distinct axial ring.

Remarks. – The original description of *H. vikensis* was drawn up in ignorance of an associated form with 18 thoracic segments, which is described here as *H. spinulosus*. The diagnosis is now revised to differentiate these two species as well as the more typical Bohemian species of *Hydrocephalus*.

The original account of the librigena of *H. vikensis* did not mention the gently backwardly convex curvature of the
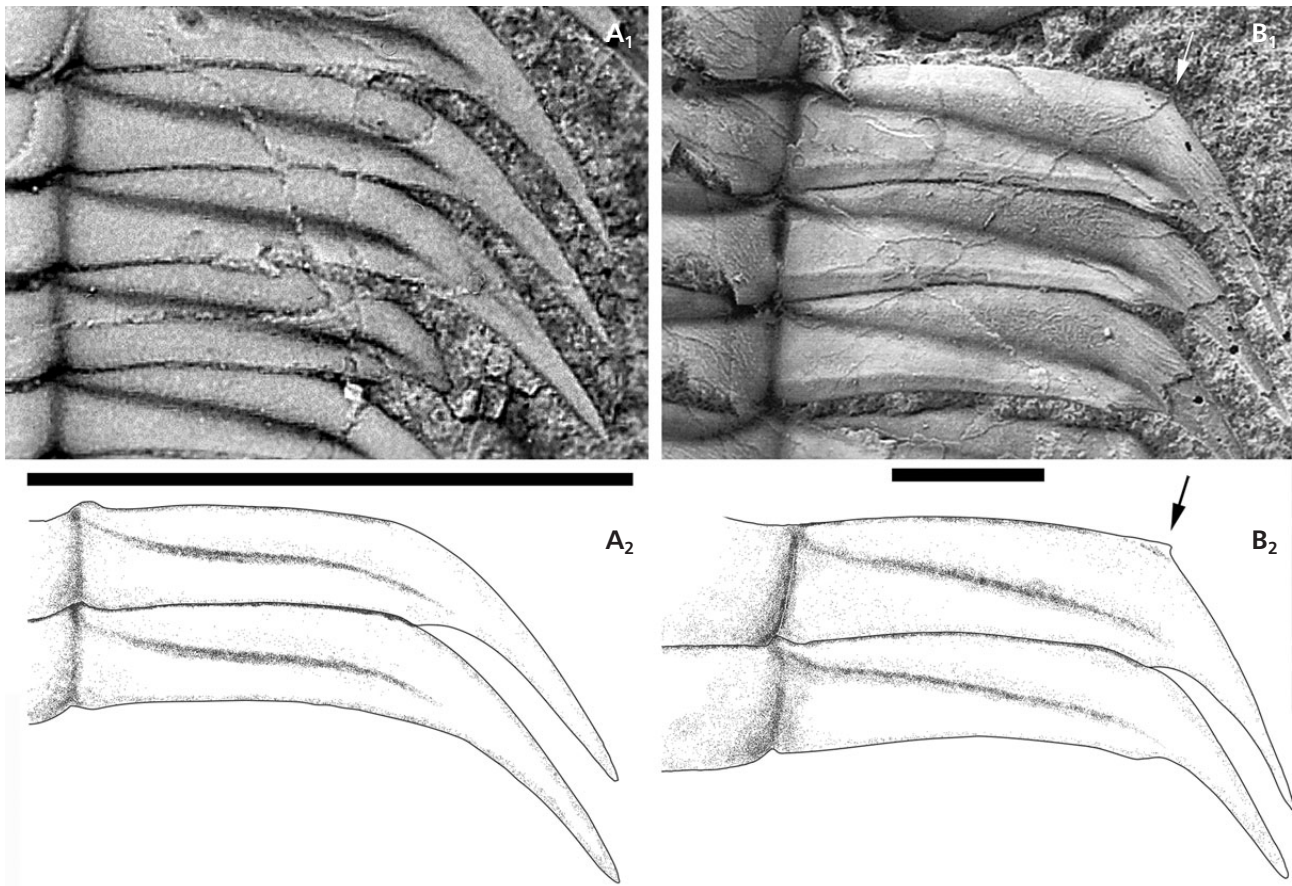
Figure 31. A$_1$, A$_2$ – *Hydrocephalus spinulosus* sp. nov. PMU 25711/37, photograph and interpretive drawing of thoracic segments 4 to 5. • B$_1$, B$_2$ – *Hydrocephalus vikensis* Rushton & Weidner, 2007. NHMUK It 29216, photograph and interpretive drawing of thoracic segments 6 to 7. The arrows point to an articulating process seen at the anterior edge of the pleura.

posterior margin; it described the posterior edge of the cephalon as forming "a roughly transverse line" (Rushton & Weidner 2007, p. 397). Although the librigenae of a well-preserved specimen on the "Big Block" (Fig. 20B) are slightly displaced, it is clear that the genal spines are slightly 'advanced' compared with the posterior margin of the cranidium. The "roughly transverse line" was mentioned because it constitutes a distinction from the Bohemian species *H. minor* and *H. carens*; the latter in particular has well advanced genal spines and the inner spine angle is acute (Barrande 1852, pl. 12, fig. 1; Šnajdr 1958, pl. 27, fig. 5).

The larger example from the "Big Block" (Fig. 20B) is about 32 mm long. The anterior pleural spines are nearly straight and the pygidium typically shows a distinct axial ring and a pair of pleural grooves. The smaller specimen (not figured, but see Fig. 4B) is incomplete. The cranidium has a narrow preglabellar field, just like a cranidium of similar size illustrated by Rushton & Weidner (2007, pl. 3, fig. 3); the pygidium is 1.3 mm long; its axis appears to have an anomalous transverse shape.

Thomas Weidner collected a large specimen of *Hydrocephalus vikensis* (Fig. 30B) from Mon, south of Viken (Fig. 2B). The cephalon is 30 mm long and shows the widest part of the glabella well forward of point γ and the thoracic segments with straight pleural spines. Part of the thorax is disarranged, but 17 thoracic segments can be discerned. The pygidium appears to be typical of the species.

Acknowledgements

References

Barrande, J. 1846. *Notice préliminaire sur le systême silurien et les Trilobites de Bohême*. 97 pp. C.L. Hirschfeld, Leipsic.

Barrande, J. 1852. *Systême Silurien du centre de la Bohême. 1ère partie. Recherches Paléontologiques, vol. 1, Crustacés, Trilobites*. xxx + 935 pp. Prague, Paris.

Bergström, J. & Levi-Setti, R. 1978. Phenotypic variation in the Middle Cambrian trilobite *Paradoxides davidis* Salter at Manuels, SE Newfoundland. *Geologica et Palaeontologica 12*, 1–40.

Chernysheva, N.E. 1971. [The Amgan Stage in the Altay-Sayan region]. *Trudy Sibirskogo naucho-issledovatel'skogo instituta geologii, geofiziki i mineral'nogo syr'ya (SNIIGGIMS) 111*, 1–267. [in Russian]

Courtessole, R. 1973. *Le Cambrien Moyen de la Montagne Noire. Biostratigraphie*. 248 pp. Imprimerie d'Oc, Toulouse.

Dean, W.T. & Rushton, A.W.A. 1997. Superfamily Paradoxidoidea, 470–481. *In* Kaesler, R.L. (ed.) *Treatise on Invertebrate Paleontology, Part O, Arthropoda 1. Trilobita, revised, Volume 1*. xxiv + 530 pp. University of Kansas & Geological Society of America, Boulder & Lawrence.

Ebbestad, J.O.R., Rushton, A.W.A., Stein, M. & Weidner, T. 2013. A paradoxidid moult ensemble from the Cambrian of Sweden. *GFF 135*, 18–29.
DOI 10.1080/11035897.2012.737365

Esteve, J. 2014. Intraspecific variability in paradoxidid trilobites from the Purujosa trilobite assemblage (middle Cambrian, northeast Spain). *Acta Palaeontologica Polonica 59(1)*, 215–240.

Fletcher, T.P., Theokritoff, G., Lord, G.S. & Zeoli, G. 2005. The early paradoxidid *harlani* trilobite fauna of Massachusetts and its correlatives in Newfoundland, Morocco, and Spain. *Journal of Paleontology 79*, 312–336.
DOI 10.1666/0022-3360(2005)079<0312:TEPHTF>2.0.CO;2

Geyer, G. 1993. The giant Cambrian trilobites of Morocco. *Beringeria 8*, 71–107.

Geyer, G. & Landing, E. 2001. Middle Cambrian of Avalonian Massachusetts: stratigraphy and correlation of the Braintree trilobites. *Journal of Paleontology 75*, 116–135.
DOI 10.1666/0022-3360(2001)075<0116:MCOAMS>2.0.CO;2

Geyer, G. & Vincent, T. 2014. The *Paradoxides* puzzle resolved: the appearance of the oldest paradoxidines and its bearing on the Cambrian Series 3 lower boundary. *Paläontologische Zeitschrift 89(3)*, 335–398. DOI 10.1007/s12542-014-0225-5

Hammer, Ø., Harper, D.A.T. & Ryan, P.D. 2001. PAST: Palaeontological statistics software package for education and data analysis. *Palaeontologia Electronica 4(1)*, 1–9. http://palaeo-electronica.org/2001_1/past/issue1_01.htm

Hawle, I. & Corda, A.J.C. 1847. Prodrom einer Monographie der böhmischen Trilobiten. *Abhandlungen der königlichen böhmischen Gesellschaft der Wissenschaften 5(5)*, 1–176.

Jegorova, L.I., Shabanov, Yu.Ya., Pegel, T.V., Savitsky, V.E., Suchov, S.S. & Chernysheva, N.E. 1982. [Maya Stage of the type locality (Middle Cambrian of the Siberian Platform)].

Mezhvedomstvennyy Stratigraficheskiy Komitet SSSR, Trudy 8, 1–146. [in Russian]

Jegorova, L.I., Shabanov, Yu.Ya., Rozanov, A.Yu., Savitsky, V.E., Chernysheva, N.E. & Shishkin, B.B. 1976. [Elankan and Kuonaman facies stratotypes at the lower limit of the Middle Cambrian of Siberia]. *Trudy Sibirskogo nauchno-issledovatel'skogo instituta geologii i geofiziki mineral'nogo syr'ya (SNIIGGIMS) 211*, 1–228. [in Russian]

Kim, D.H., Westrop, S.R. & Landing, E. 2002. Middle Cambrian (Acadian Series) conocoryphid and paradoxidid trilobites from the upper Chamberlain's Brook Formation, Newfoundland and New Brunswick. *Journal of Paleontology 76*, 822–842.
DOI 10.1666/0022-3360(2002)076<0822:MCASCA>2.0.CO;2

Münder, U. 2007. Hundert auf einen Streich. Neue Paradoxiden von Jämtland. *Fossilien. Zeitschrift für Hobbypaläontologen, 24*, 143–148.

Öpik, A.A. 1967. The Mindyallan Fauna of north-western Queensland. *Bureau of Mineral Resources, Geology and Geophysics, Bulletin 74*, 2 vols, xvi + 404 pp. and 166 pp.

Orłowski, S. 1965. A revision of the Middle Cambrian fauna from the Słowiec Hill (Holy Cross Mountains). *Biuletyn Geologiczny Uniwersytetu Warszawskiego 6*, 134–146.

Orłowski, S. 1985. New data on the Middle Cambrian trilobites and stratigraphy in the Holy Cross Mts. *Acta Geologica Polonica 35*, 251–263.

Rushton, A.W.A. & Weidner, T. 2007. The Middle Cambrian paradoxidid trilobite *Hydrocephalus* from Jämtland, central Sweden. *Acta Geologica Polonica 57*, 391–401.

Savitsky, V.E, Evtyshenko, V.M., Jegorova, L.I., Kontorovich, A.E. & Shabanov, Yu.Ya. 1972. [Cambrian of the Siberian Platform]. *Trudy Sibirskogo nauchno-issledovatel'skogo instituta geologii i geofiziki mineral'nogo syr'ya (SNIIGGIMS) 130*, 1–200. [in Russian]

Šnajdr, M. 1957. O nových trilobitech z českého kambria. *Věstník Ústředního ústavu geologického 32*, 235–244.

Šnajdr, M. 1958. Trilobiti českého středního kambria. *Rozpravy Ústředního ústavu geologického 24*, 1–280.

Šnajdr, M. 1987. The genera *Paradoxides* Brongniart and *Hydrocephalus* Barrande (Trilobita). *Věstník Ústředního ústavu geologického 62*, 97–104.

Šuf, J. 1926. O českých Paradoxidech se zvláštním zřetelem k jejich vývoji (Développement des Paradoxidés Tchèques). *Sborník Státního geologického ústavu Československé republiky 6*, 31–67. [in Czech and French]

Weidner, T. & Ebbestad, J.O.R. 2011. New 'Paradoxides' species from the Middle Cambrian of Jämtland and Ångermanland, Sweden. *GFF 133*, 73.

Weidner, T. & Ebbestad, J.O.R. 2014. The early middle Cambrian agnostid *Pentagnostus praecurrens* (Westergård 1936) from Sweden. *Memoirs of the Association of Australasian Palaeontologists 45*, 403–419.

Weidner, T. & Nielsen, A.T. 2015. *Agraulos longicephalus* and *Proampyx? depressus* (Trilobita) from the Middle Cambrian of Bornholm, Denmark. *Bulletin of the Geological Society of Denmark 63*, 1–11.

WEIDNER, T., RUSHTON, A.W.A. & EBBESTAD, J.O.R. 2014. A paradoxidid-agnostoid fauna from the mid-Cambrian (Stage 5) of the Caledonian Lower Allochthon on Tåsjöberget, Ångermanland, Sweden. *GFF 136*, 513–530. DOI 10.1080/11035897.2014.888471

WESTERGÅRD, A.H. 1936. The Paradoxides oelandicus Beds of Öland. *Sveriges Geologiska Undersökning C 394*, 1–66.

WESTERGÅRD, A.H. 1953. Non-agnostidian trilobites of the Middle Cambrian of Sweden, III. *Sveriges Geologiska Undersökning C 526*, 1–58.

WHITTINGTON, H.B., & KELLY, S.R.A. 1997. Morphological terms applied to Trilobita, 313–329. *In* KAESLER, R.L. (ed.) *Treatise on Invertebrate Paleontology, Part O, Arthropoda 1. Trilobita, revised, Volume 1*. xxiv + 530 pp. University of Kansas & Geological Society of America, Boulder & Lawrence.